CZECH TECHNICAL UNVERSITY IN PRAGUE
Faculty of Electrical Engineering
Department of Circuit Theory

Matrix of four quadrants slot applicators for microwave thermotherapy

Diploma thesis

Supervisor: Prof. Ing. Jan Vrba, CSc.
Student: Bc. Nina Kejzlarová

May 2014

Czech Technical University in Prague
Faculty of Electrical Engineering

Department of Circuit Theory

DIPLOMA THESIS ASSIGNMENT

Student: Bc. Nina K e j z l a r o v á

Study programme: Biomedical Engineering and Informatics

Specialisation: Biomedical Engineering

Title of Diploma Thesis: Matrix of Four Quadrant Slot Applicators for Microwave Thermotherapy

Guidelines:

The goal of this project is a basic design of a planar applicator for microwawe thermotherapy. This applicator will be created by a matrix of four mutually separated quadrant resonators based on technology of slotted transmission lines. Further step is optimization of the discussed applicator by aid of EM field simulator SEMCAD X with respect to best possible impedance matching and best possible 3D homogeneity of SAR distribution.
Your task is then to implement this applicator and to verify it experimentally by heating agar phantom. Technical specification: frequency 434 MHz, input power 100 W, the reflection coefficient of the discussed applicator less than 0,1.

Experimental evaluation of the applicator:

- Measure the reflection coefficient of the discussed applicator on agar phantom, which simulates the dielectric and thermal parameters of muscle tissue.
- Measure 3D distribution of SAR of matrix of tested applicators on agar phantom by aid of an infrared camera.

Bibliography/Sources:

[1] Vrba, J.: Lékařské aplikace mikrovlnné techniky. Skriptum ČVUT, Praha, 2007
[2] Int. Journal of Hyperthermia, ESHO 1992 – 2012.

Diploma Thesis Supervisor: prof. Ing. Jan Vrba, CSc.

Valid until: the end of the summer semester of academic year 2013/2014

L.S.

prof. Ing. Pavel Sovka, CSc.
Head of Department

prof. Ing. Pavel Ripka, CSc.
Dean

Prague, February 17, 2014

České vysoké učení technické v Praze
Fakulta elektrotechnická

Katedra teorie obvodů

ZADÁNÍ DIPLOMOVÉ PRÁCE

Student: Bc. Nina K e j z l a r o v á

Studijní program: Biomedicínské inženýrství a informatika (magisterský)

Obor: Biomedicínské inženýrství

Název tématu: Matice čtyř kvadrantních štěrbinových aplikátorů pro mikrovlnnou termoterapii

Pokyny pro vypracování:

Vaším úkolem je navrhnout a pomocí simulátoru EM pole SEMCD X optimalizovat matici čtyř kvadrantních štěrbinových planárních rezonátorů pro funkci aplikátoru pro lokální termoterapii. Plošné uspořádání těchto rezonátorů volte s ohledem na homogenitu rozložení veličiny SAR a na efektivní hloubku profilu veličiny SAR.
Dále je vaším úkolem navrženou matici štěrbinových planárních rezonátorů realizovat a experimentálně ověřit na planárním agarovém fantomu. Technická specifikace: frekvence 434 MHz, příkon 100 W, činitel odrazu matice intersticálních aplikátorů menší než 0,1.

Testování aplikátoru:

- změřte činitel odrazu matice testovaných aplikátorů navázaných na agarový fantom, který simuluje dielektrické a teplotní parametry svalové tkáně,
- změřte 3D distribuci SAR matice testovaných aplikátorů navázaných na agarový fantom, a to pomocí infračervené kamery.

Seznam odborné literatury:

[1] Vrba, J.: Lékařské aplikace mikrovlnné techniky. Skriptum ČVUT, Praha, 2007
[2] Int. Journal of Hyperthermia, ESHO 1992 – 2012.

Vedoucí diplomové práce: prof. Ing. Jan Vrba, CSc.

Platnost zadání: do konce letního semestru 2013/2014

L.S.

prof. Ing. Pavel Sovka, CSc.
vedoucí katedry

prof. Ing. Pavel Ripka, CSc.
děkan

V Praze dne 17. 2. 2014

Affirmation

I confirm that I wrote the Master thesis *Matrix of four quadrants slot applicators for microwave thermotherapy* based on my individual efforts and I used to complete a list of the references that I mention in the list annexed to the thesis in accordance with Methodological guideline number 1/2009 on the observance of ethical principles in the preparation of university thesis.

In Prague on 12 May 2014 .....

Signature

Abstract

The Diploma thesis *Matrix of four quadrants slot applicators for microwave thermotherapy* is a practical assignment which should primarily form a basis for properly working product.

In chapters 2 and 3 I deal with a theoretical analysis of the influence of the electromagnetic field on biological tissue and with description of the principle, the progress and the results of cancer treatment by means of hyperthermia.

The two following chapters include summary of information about planar applicators for subsurface treatment. Further I continue with comparison and description of impact of voxel's number or different shape of slot on results, description of optimization of one quadrant and then finally process of optimization and description final matrix applicator in environment of a simulator for electromagnetic field SEMCAD.

The reached and measured results including evaluation of the whole thesis are mentioned in the final chapters.

Abstrakt

Diplomová práce "*Matice čtyř kvadrantů štěrbinových aplikátorů pro mikrovlnou termoterapii*" je praktickou úlohou, jejímž výsledkem je především správně fungující výrobek.

V kapitolách 2 a 3 se věnuji teoretickému rozboru vlivu elektromagnetického pole na biologickou tkáň a popisu principu, průběhu a výsledků léčby nádorového onemocnění pomocí hypertermie.

Dvě následující kapitoly obsahují souhrn informací o planárních aplikátorech pro podpovrchovou léčbu. Dále pokračuji s porovnáními a popisem vlivu množství použitých voxelů nebo rozdílnosti tvaru štěrbiny, popisem optimalizace jednoho kvadrantu a nakonec s postupem optimalizace finálního maticového aplikátoru v prostředí simulátoru elektromagnetického pole SEMCAD.

Dosažené a naměřené výsledky včetně zhodnocení celé práce uvádím v závěrečných kapitolách.

Acknowledgements

I would like to express my special gratitude to my supervisors of Diploma thesis Prof. Ing. Jan Vrba, CSc. and Associate Professor Dr. Felipe L. Peñaranda-Foix for professional guidance and useful advice during the creation of my work. Then I would like to thank for useful comments and advice and for supervision by during the final measurement to Ing. Ondřej Fišer and Ing. Ilja Merunka I also thank to Ing. Viktor Adler for expert supervision and assistance in the production of planar applicator. Then I thank to Mgr. Ondřej Šváb for correction of the English language. Last but not least, I thank my sister Ing. arch. Dana Kejzlarová for assistance in creating images in the environment of program ArchiCAD, and finally all my family for their support during the study.

Content

1 Introduction

We can say that the microwaves are everywhere around us. There are countless possibilities of their use. The most common way of use is transfer of information, in the fields such as industry, communications, mobile phones, satellite navigation systems, radar, satellite radio and television broadcasting. But it is also possible to use them for health treatment or diagnostic aims. In the case of diagnostic the microwaves are primarily found in imaging systems (microwaves tomography), sensors, as well as angioplasty in cardiology.

As suggested by the title of my thesis, another use of microwaves concerns heating. Heating, essence of which is the absorption of microwaves, is used to thermocoagulation in urology, in surgery, like rehabilitation in diathermy and not least in oncology to treat certain tumors called *microwave hyperthermia*. [1] My thesis is based on the principles and issues of microwave hyperthermia.

Despite the number of fields where we can meet microwaves today, microwaves are still considered relatively "young" discoveries. The first persons, who described them were J. C. Maxwell and H. Hertz in the end of 18th century [1]. But history of waveguides is much younger, first experiments with them were performed in 1932. In case of hyperthermia it was not until last 20 - 30 years [19], when there was a development in utilization of microwaves to treat tumors [2].

From the physical viewpoint, microwaves belong to electromagnetic radiation with frequency between 300 MHz and 3 THz. Therefore we speak about high-frequency radio waves. Their wavelengths range between 1 m and 0,1 mm and are significantly affected by value of relative permittivity and permeability of environment, where they are excited. [2] The other important feature is the fact, that they are completely reflected from metal objects whereas in case of other materials containing water (except in the case of distilled water), such as food or human tissue, the microwaves are effectively absorbed and converted into heat. [3]

Considering the task of my thesis, my work is not only theoretical description of microwaves and hyperthermia, but also presentation of design and optimized planar applicator in simulator of electromagnetic field SEMCAD, realized this applicator and perform with this product measurement on the model of human tissue, on agar. I divided my work into several chapters according to logical parts. In first two chapters I begin with theoretical introduction to clarify the issue of hyperthermia. In following chapter I describe from theoretical viewpoint types of planar applicators, waves, which can be excited in these applicators and parameters, which define conduction. The longest chapter, the fifth one, concerns practical work in SEMCAD and description of my workflow by design and optimized my own applicator. In the last part, I describe work progress in practical measurements with applicator and at the end I summarize all the results in the conclusion.

2 Influence of electromagnetic field on the biologic tissue

We are in room full of electromagnetic waves, our body is able to absorb almost all of waves impacting on our body. What is decisive for absorption of the waves is, among others, wavelengths of these waves. Depending on the wavelength we can speak about two kinds of waves – active and passive waves [9]. If the wavelength is longer than human body or other irradiated object then it will be not absorbed. In the same case of radio waves which can pass over the hills and propagate through the nature without termination because their wavelength can be in units of kilometers. Conversely, if the wavelength of wave is smaller or comparable with irradiated object, then the wave is being absorbed.

Reaction of human body of electromagnetic field and waves is on the level of molecules and atoms in tissues. These elements or charged particles are deformed. [1] It leads to deviation from their equilibrium position and to origin of dipoles. We call this process "polarization of dielectric" [2]. Moreover it leads to numerous changes or influence of polarization of membranes of molecules and resonation of all molecules. Among others the radicals are released.

Depending on the amount of the power density which is being absorbed we distinguish two types of influence of microwaves in terms of physiology – thermal and non-thermal effects. The limit value, which is the threshold for non-thermal effects, is given between 0,1 – 1 W/m^2 [11]. Exceeding of this limit leads to heating of tissues and manifestation of thermal effects. Absorbed density of power over 2 W/m^2 can have negative effect and is deemed detrimental and risky. If the receiving of power density is higher than 100 W/m^2, the waves can have destructive consequences for biological tissues [3].

Temperature which can tolerate the human body constantly ranges about 43,5 °C. High temperatures over 53 °C lead to coagulation, thermal drying of tissue, and temperatures over 60 °C create denaturation of proteins in tissue, which is irreversible degenerative change in tissue, because proteins are losing their biological activity [3].

There are a lot of factors which influence the interaction between electromagnetic field and irradiation material. The first group – physical factors comprise for example frequency and intensity of the radiation, duration or time of exposure and spectrum of excitation signal. The second group comprises characteristics of biological tissue such as the mass, properties of the surface, arrangement and thickness of the layers, characters of these layers, permittivity, permeability, impedance and conductivity of biological tissue [1], [2], [9], [10].

2.1 Thermal effects of microwaves

As I already mentioned above, the size of the power density which is being absorbed and which is higher than 1 W/m^2 [11] leads to the thermal effects of microwaves. But there are more parameters which are influencing of result temperature of the tissue. Very important is depth to which wave penetrates. We can affect this parameter mainly by changing of working frequency. It is accepted that with increasing frequency the depth of penetration of wave decreases. Therefore, if we want warm up surface layers, we have to use the lower frequencies and conversely.

2.2 Non-thermal effects of microwaves

Some negative effects of microwave on organism, such as fatigue, inattention, poor memory, dizziness, headache, insomnia, in extreme cases hair falling, were recorded in connection with microwaves [7], [8]. These symptoms are more subjective and individual and their cause may be, but may not be microwaves. But although we cannot feel changes of temperature during of radiation on our body, ionic currents start to flow inside the cells. It leads to changes of permeability and excitability of cell membranes and it may have adverse impact on the nervous and cardiovascular systems, for example increasing of blood pressure [7]. The doses of radiation are cumulated in the body. In regard to, mutagenic or harmful effects of microwaves on enzymes, DNA, cell membrane, or any other part of the cell haven't been demonstrated [7], this topic has been the subject of many scientific studies.

3 Thermotherapy by microwaves, hyperthermia

Cancer together with circulatory diseases are the two most common causes of death in Europe. There are a lot of oncology centers for treatment of cancer with high quality level. The level of medicine is constantly increasing. Nevertheless, in many causes of cancerous disease the most modern medicine can't be successful.

Hyperthermia is other kind of cancer treatment. The dint of microwave heating, uses the difference in thermoregulatory characteristics between healthy cells and tumor cells [1], [2], [7]. It is paradox that with increase of proportions and stage of tumor the influence and positive effect of hyperthermia's treatment increases also. The reason is degeneration and weakening the blood supply and flow, which has important influence on heat transfer away and the result is that heat in tumor tissue is increasing faster than in health tissue around [11], [14], [19].

The principle of hyperthermia's treatment is increase of the temperature of tumor tissue to the range 42 – 45 °C [18], due to the absorption of microwaves. Temperatures below 42 °C do not have influence on physiology of both types of tissue. Temperatures over 45 °C are very dangerous to healthy tissue near tumor tissue. The cells of healthy tissue would be damaged, what is by treatment more than undesirable, and the treatment would become counterproductive [8]. Healthy tissue fights high temperature due to good blood supply better than tumor tissue. Therefore by temperature around 43 °C the temperature in healthy tissue begins to fall due to transfer of heat away, but the temperature in tumor tissue continues to rise [1], [20], as shown in the graph (Picture 3-1) below.

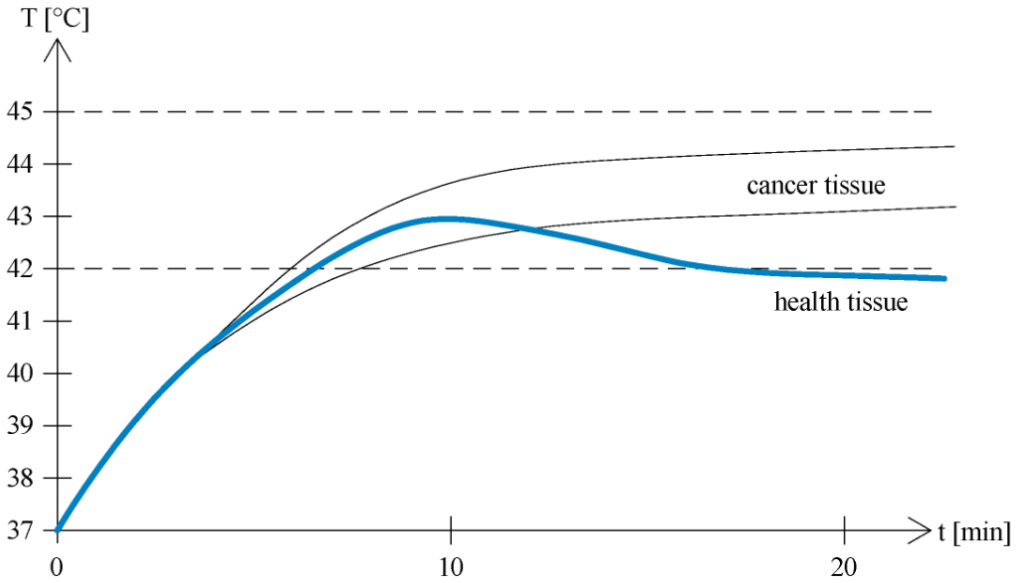

Picture 3-1 Graph of during of temperatures in tumor and health tissues [1].

Hyperthermia has no side secondary carcinogenetic effects and therefore is preferred often in pediatric oncology. Other possibilities for using this kind of treatment are for patients who suffer from cancerous disease which is resistant to conventional radiotherapy, such are sarcomas and melanomas, tumors at an advanced stage, encapsulated tumors, or otherwise fixed tumors or during repeated occurrence [1], [3].

To increase of treatment's efficiency hyperthermia is combined with conventional radiotherapy. As the first step the patients undergo the radiotherapy, where the tumor contracts and retreats [1]. The blood flow decreases and, consequently, hyperthermia is more effective. In the reverse order, with hyperthermia like first step, we could damage the patient because upon increase of temperature in tissue the blood flow increases and therefore the susceptibility of health tissue to radiation increases, as well [8].

One of the technical parameters of hyperthermia systems is working frequency where short waves, very short waves or microwaves are used. For treatment we can use frequencies in range between 13,56 MHz and 5,80 GHz, with permitted deviation from this values is 0,05 % [1], [2]. The most common power of systems is between 20 and 400 W [1]. Therapeutic dose D_t, which is received by the patient, is checked during the exposition. We can calculate this dose very simply, namely by multiplying power P and time of radiation t, physical unit is therefore watt-second [W·s] [1], [8].

$$D_t = P \cdot t \quad [W \cdot s] \tag{3. 1}$$

3.1 Box diagram of application of hyperthermia in practice

The entire system is controlled and managed by a specialist through the control computer. The computer is connected with a microwaves power generator. The power from generator is supplied to planar applicator by microwaves wiring, such as coaxial cable (two concentric cylindrical conductors isolated by dielectric) [4]. This power is emitted from planar applicator into the surrounding area in form of electromagnetic energy. This radiation is distributed on both sides of applicator [6]. In the picture (Picture 3-2) we can see a layer of water (water bolus). This layer protects a skin of patient against formation of hot localities and burns [1], [20]. In the following picture we can see also how microwaves are absorbed under the skin and how the temperature is distributed. The sensors are used for control of temperature (up to 8 sensors in practice) [1]. The sensors are situated close to the heated area. In practice sensors are often placed under the skin in the irradiated area. We can obtain more accurate data about progression of temperature in the given area, but this intervention is usually painful for the patient. Computer is processing information from sensors and we can see them in form of graph on the display and depending on them we can change the power, which is going from generator, so that that the temperature was ranged within the prescribed limits [1].

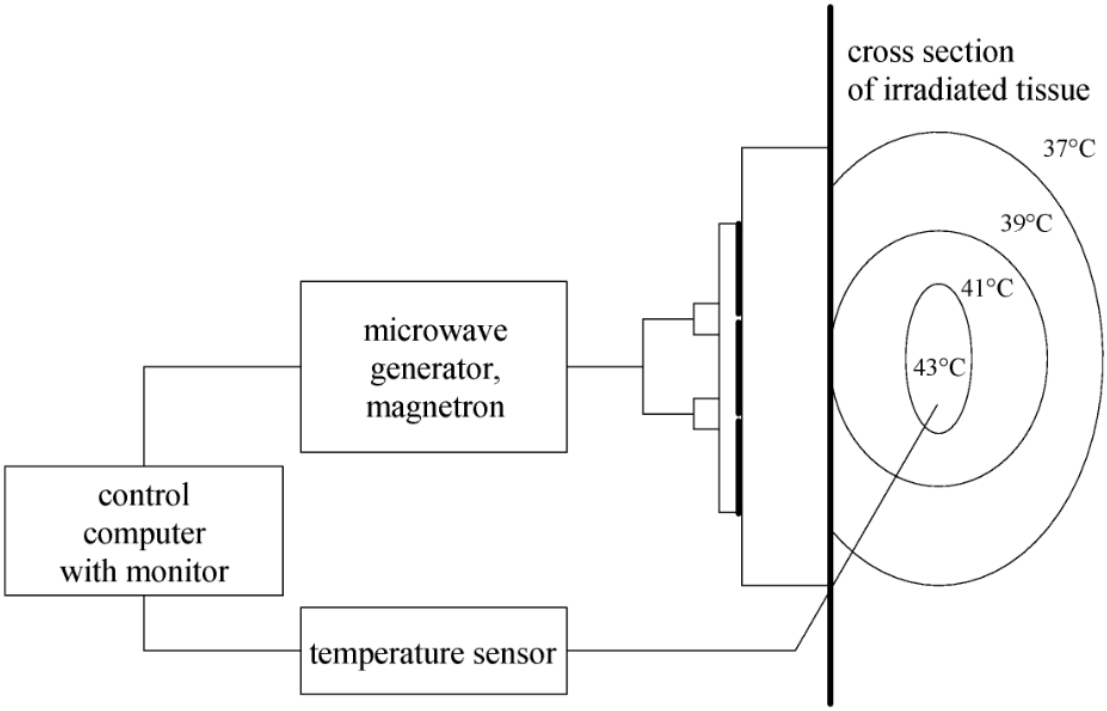

Picture 3-2 Box diagram of hyperthermia's system during the treatment [1].

3.2 Microwaves power generator

Magnetron is the most common type of microwaves power generator. Anode is a hollow cylinder from ferromagnetic magnet with even number of cavity resonators [12]. The space in anode is filled with vacuum a cathode is in the middle. The flow of electrons emitted from the cathode is accelerated by a strong magnetic field. This flow of electrons indicates microwaves inside of cavity resonators. Microwaves are transferred by waveguide. Cross section of magnetron you can see in the picture (Picture 3-3) below [12].

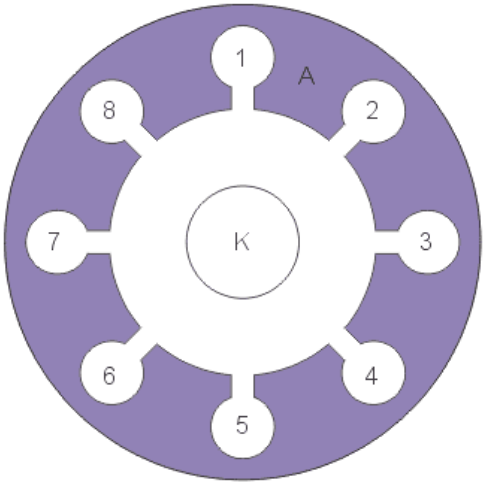

Picture 3-3 Cross section of magnetron (K – cathode, A – anode) [12].

3.3 Practical use

During the professional practice at the bachelor's level at the university I had the opportunity to participate in the application of hyperthermia on patient which occurred in the Institute of Radiation oncology in University Hospital Bulovka in Prague. This was a patient after complete ablation of the breast, when it failed to remove all of tumor tissue and tumor started growing up again. The patient had combined therapy radiotherapy and hyperthermia together. Already after second application the doctor could constant significant positive effect and retreat of tumor tissue. Many expert studies confirm these results and from the majority of them we can read that this combined therapy increases more than by half the percentage of success compared with radiotherapy alone in many causes [1]. Progress of treatment by using hyperthermia we can see in the pictures (Picture 3-4 a), b) and c)) below.

Picture 3-4 a) (left) tumor before treatment, b) (middle) tumor after treatment c) (right) place of the former tumor at intervals of approximately two months after the end of treatment [1].

4 Planar applicators for subsurface treatment

Planar applicators are plane structures which we classify as microwave circuits. Mostly they achieve of small dimensions, which is one of their main advantages. They include plate from dielectric material, for example from cuprextite or from many others, and from very thin metallic layer covering this dielectric plate from one side or from both sides. The planar structures include microstrip line, symmetric stripline, slotline, coplanar waveguid, grounded coplanar waveguide and coplanar strips [8], all of these structures are shown in the following picture (Picture 4-1 a) – f)).

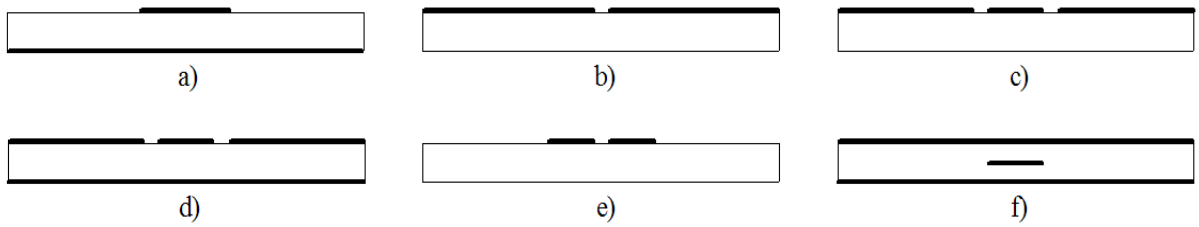

Picture 4-1 a) microstrip line, b) slotline, c) coplanar waveguid, d) grounded coplanar waveguide, e) strips and f) symmetrical stripline [8].

Their positive characteristics are [1], [2], [8], [10]:

- already referred small dimensions and also their low weight
- low production costs (low material consumption, low complexity and simplicity of manufacture of applicators)
- high bandwidth – antennas change their electrical properties, such as impedance or distribution of radiation very significantly and in relatively wind band of frequency. (The requirement on input impedance is that the parameter of standing waves PSV should not exceed the 2)
- reliability and stability of parameters
- easy combination with other constructional elements (for example: semiconductor structural elements)

Their disadvantages compared with waveguides are [1], [7], [9], [10]:

- worse values of parameters like as attenuation, factor of quality of circuits or the transmitted power

- necessity of heat transfer away and this more by structures without metal layer on back side such as for example by slot-line or coplanar line, when the applicator is radiating to both sides, which is undesirable with respect to the safety of operators
- high requirements of quality of manufacture of applicators and less possibilities for additional tuning of circuits

4.1 Types of planar applicators

As mentioned above, there are many types of structures of planar applicators. In the following paragraphs I will describe the most common types used in practice.

4.1.1 Micro-strip line

This structure includes metal conductive layer of various shapes, for example a square or a circle (according to the requirements on radiation) on the dielectric plane, we can call it "patch". The dielectric plane is 0,1 – 3 mm thick and value of permittivity ε_r is to 10, depending on the material (for example teflon 2,1, cuperxtit 4, corundum 10 and special ceramic materials to 30) [5]. The plane has to be metallized on the other side or connected to conductive material. This arrangement serves as a counterweight. We can excite the patch with coaxial cable or with thin metallized strip, micro-strip line [6].

In the pictures (Picture 4-2 a) – c)) below we can see structures of micro-strip line.

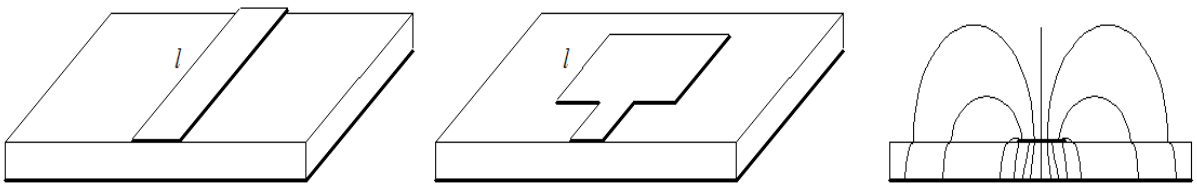

Picture 4-2 a) (left) micro-strip lead, b) (in the middle) structure of patch and c) (right) electromagnetic field distribution [1], [4].

The most important and critical parameter in this case is length of micro-strip l [m]. Provided that one of the dimensions is significantly greater than the other and resultant form of patch is rectangle, than length of strip is approximately one half of wavelength in dielectric λ_g [6]:

$$l = 0{,}49\lambda_g = 0{,}49 \cdot \left(\frac{\lambda}{\sqrt{\varepsilon_r}}\right) \quad (4.\ 1)$$

Where λ – length of wave in vacuum and ε_r – value of relative permittivity of dielectric plane.

But more common is patch with form of square with edge length corresponding to quarter of the wavelength or the entire one wavelength in dielectric (in the second cause we have to powering this patch in the middle of length of this structure *l*) [1], [6].

$$l = \frac{\lambda_g}{4}\ ;\ \text{or}\ \ l = \lambda_g \quad (4.\ 2)\ (4.\ 3)$$

The advantage of these antennas is their metal layer on their back side, which causes these structures to radiate only on one side, another side is shielded.

4.1.2 Coplanar waveguide

This line consists of three conductors on one side of dielectric plane, in other words, we can say that this lead is open. Back side of plane is not metallized, like a counterweight or ground here are working two outers conductors and wave is propagated along the middle the conductive strip [8]. Then electrical field has distribution symmetrical along the axis of the middle conductive strip.

The problem of these structures of antennas is distribution of energy to both sides of plane, which is undesirable with respect to the safety of operators, as mentioned above among the disadvantages of planar antennas.

4.1.3 Slot-line

These structures are composed from two metallized sheets separated by non-conductive slot or very thin gap up on the dielectric substrate. The plane, as in the case of coplanar conduction, is not metallized on the other side. Width of the slot is significantly smaller than width of the metallized sheets and, at the same time, significantly smaller allowing the wave to propagate through the lead [6]. The most common length of slot is one half of wavelength. Wave that is propagated in slot is of type HEM (H≠0) and has properties of surface wave [4].

We can eliminate the disadvantage of distribution of energy to both sides of plane by increasing of permittivity of the support plate.

Subject of my thesis is applicator for hyperthermia, structure of which includes the right to slot-conduction. In my bachelor thesis I was designating applicator as two concentric squares separated by non-conductive slot whose average length was equal to one wavelength of the wave. We can see the layout of this slot-structure in the following picture (Picture 4-3).

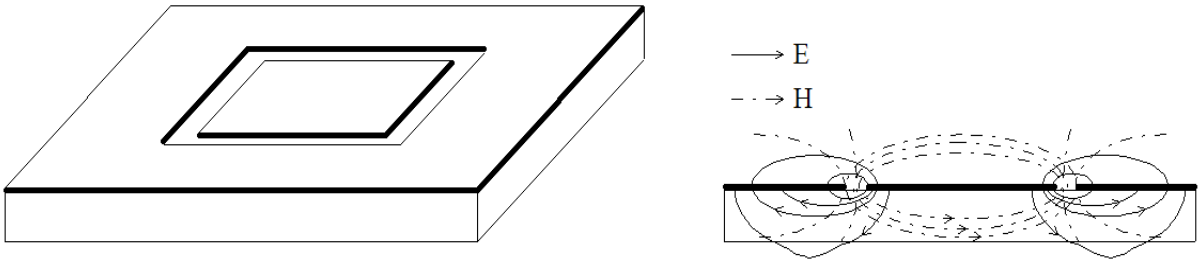

Picture 4-3 a) (left) structure of slot-line from my bachelor thesis and b) (right) distribution of electromagnetic field in this structure [1], [4].

In this work I will focus on a similar structure but the difference will be in shape of the slot. It the case at hand, it will not form a regular square, but a circle divided into four sectors. The length of the slot will be also equal to one wavelength of the wave. We can see the shape of this irregular structure in the following picture (Picture 4-4).

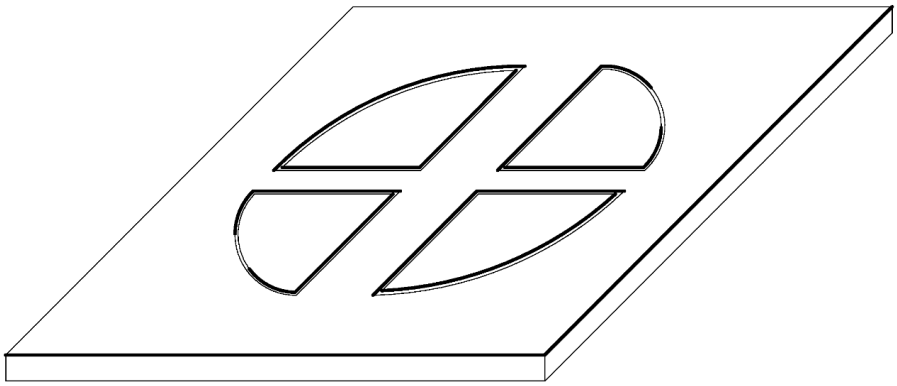

Picture 4-4 Structure of slot-line of diploma thesis.

4.2 Waves emerging in the planar conduction

We can classify the waves emerging and propagating on the surface of planar applicator into three groups depth waves, surface waves and reflected waves. Reflected waves are completely unwanted and we try to avoid them. During the modeling and suggesting of applicator is this parameter, parameter of the ratio of reflected waves, significantly important [1], [2]. Surface waves propagate along the surface of patient's body, tissue is heated by them only into a very small insignificant depth and they can cause on the body of the patient to create so-called "hot places"[11]. Therefore, waves which we try excite on planar conduction or planar applicator, are depth waves.

4.2.1 The depth waves

The depth of the tissue into which the waves penetrate is determined primarily by working frequency on basis of which applicator radiates and impedance matching of applicator. It is accepted that with increasing frequency the depth of penetration of waves decreases and vice versa [4]. Others parameters influencing the depth of penetration of waves is size of the aperture of applicator and the distribution and type of biological tissue.

Frequency of 2,45 GHz is used for surface application. In this case, waves penetrate the tissue and heat up the tissue approximately 1,5 cm under the skin [11]. We use this therapy if same important bodily organ under the tumor is threatened by the intervention of waves. This can happen for example when we are radiating tumor located on the neck, where we have to be very careful not to affect the brain.

In contrary to heating of tissue at greater depths around 4 – 8 cm, it is necessary to use much lower frequency. Applicators for this kind of treatment are designed for the working frequency 13,56 MHz or 27,12 MHz [1], [2].

The applicator, which I design and produce, will function at the frequency 433,92 MHz (zone 434 MHz). By this frequency we can assume that heating of biological tissue will propagate to depth of 2 – 4 cm [9].

In planar structures we try to excite only the TEM waves, which are characterized by the ability to propagate through smaller dimensions of conduction and simplicity of distribution of electromagnetic field. Structure of electromagnetic field in the TEM wave corresponds to an electrostatic field [4]. We try to eliminate other types of waves that may occur, for example waveguide waves TE and TM.

4.2.2 Wave TEM in the line

The TEM waves are transversal electromagnetic waves for which it is typical that both longitudinal components, electrical and magnetic component of field are equal to zero: $E_z = 0$ i $H_z = 0$ [4].

Vectors of intensity *E* and *H* and field lines are also localized in a transverse plane to the direction of propagation. This ensures that waves propagate deep in the tissue. Provided that the vector E is perpendicular to the body surface, the wave would be absorbed already upper layer of the tissue (adipose tissue). This could result in overheating and formation of "hot places" [1].

The most typical and the most common conduction or line of the TEM wave is coaxial cable. These are two concentric conductors in the form of coaxial cylinders between them is low-loss dielectric material [1], [4].

In the following pictures (Picture 4-5 a) and b)) there is a sketch of cross section of coaxial cable with clearly marked distribution of electromagnetic field of the TEM wave.

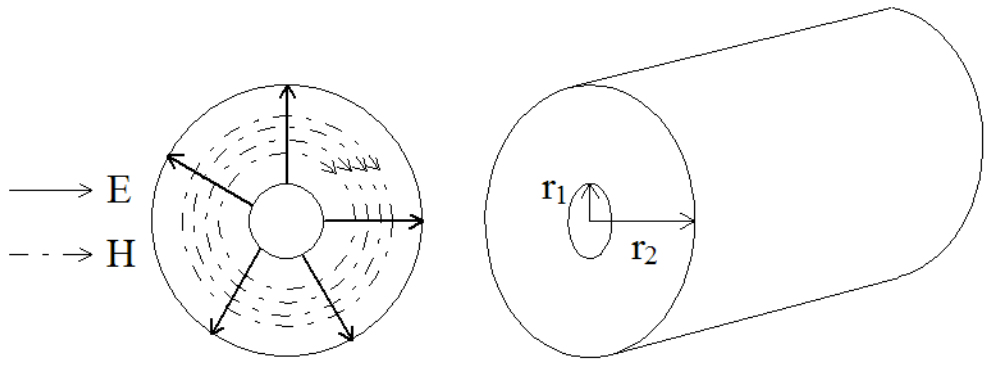

Picture 4-5 a) (left) the distribution of electromagnetic field of wave TEM in the conduction and b) (right) cross section of coaxial cable [1], [4].

Electric and magnetic field of the TEM wave in this kind of conduction corresponds to the electrostatic field between charged conductors and magnetic field of wires, by which the electric current flows.

4.3 Parameters defining conduction

Parameters determining the basic characteristics of conduction are the constant of propagation k, the wave impedance Z_0, the coefficient of reflection R, standing wave ratio (SWR)), Specific absorption rate (SAR), and effective penetration depth d [1], [7], [8], [20].

4.3.1 Transfer coefficient

The constant of propagation in conduction k can be expressed as [1]:

$k = \beta - j\alpha$, (from Helmholz equation we know that: $k^2 = -\gamma^2$) (4. 4)

β – phase constant [rad/m(length)], α – attenuation [dB/m].

The characteristic impedance is defined as the ratio of intensities of transverse components of the electric and magnetic fields that are propagated from the source.

4.3.2 The wave impedance

Wave impedance Z_0 can be defined as the fraction of the intensity of electric field E and intensity of magnetic field H [2]:

$$\mathrm{Z} = \frac{\mathrm{E}}{\mathrm{H}} \tag{4. 5}$$

Where E is intensity of electric field and H is intensity of magnetic field.

4.3.3 The coefficient of reflection

We can calculate the coefficient of reflection in a place of electric load R_z from impedance in a place of electric load Z_z and impedance at the beginning of conduction Z_0 [1], [7]:

$$R_z = \frac{Z_z - Z_0}{Z_z + Z_0} \tag{4. 6}$$

Ideally, the value of the reflection coefficient R_z is equal to 0: $R_z = 0$, so $Z_z = Z_0$, then the wave does not reflect and we can say that the conduction is adapted [2].

Provided that the wave is reflected off the tissue, this reflected wave consists with a gradual wave and together form a standing wave. Rate of formation of standing waves can be expressed by the standing wave ratio (SWR) [11].

4.3.4 The ratio of standing waves

SWR is a scalar variable whose value is always greater than one and is determined by fraction of the voltage at the maximum, or flick of wave U_{max} to the voltage at the minimum, or node of the standing wave U_{min} [1].

$$SWR = \frac{U_{max}}{U_{min}} = \frac{1 + |R|}{1 - |R|} \tag{4. 7}$$

Where R is the coefficient of reflection.

4.3.5 Specific absorption rate

SAR – specific absorption rate is defined as absorbed power of electromagnetic wave in 1 Kg of tissue [W/kg]. It is time derivation of increment of energy, which is absorbed in tissue with certain volume and density. SAR describes very accurately the exposure of tissue, but it is very difficult to measure it [8]. According to the norms (ANSI – American national standard institute and European Union) value of SAR must not exceed limit 0,4 W/kg (which is a tenth of the value meaning increasing the temperature of the exposed tissue) [1], [2].

The simplest expression of SAR is share of power of electromagnetic wave P and the product of density ρ and tissue volume V (this product represents mass of volume V) [7]:

$$SAR = \frac{\partial P}{\rho \cdot \partial V} \ \text{[W/kg]} \tag{4. 8}$$

Further we can use the spatial distribution of the electric field *E(x,y,z)* [8]:

$$SAR = \frac{\sigma}{\rho}\frac{|E(x,y,z)|^2}{2} \tag{4. 9}$$

Where σ is electrical conductivity of the tissue (the most common value is reported σ = 0,8 S/m) and ρ is density of tissue.

Or we can use the spatial temperature distribution *T(x,y,z,t)*, in case of neglecting heat conduction in the body [1], [7]:

$$SAR = c \cdot \frac{\Delta T(x,y,z,t)}{\Delta t} \tag{4. 10}$$

Where c is specific heat of tissue and t is time.

4.3.6 Effective penetration depth

The depth, to which electromagnetic waves penetrate the tissue is determined and affected by frequency of this wave. The lower the frequency of the wave is, the more deep the wave penetrates into the tissue. Furthermore, the depth of penetration affects the size of the aperture of the applicator and the tissue properties, particularly its spatial distribution [2]. For simpler calculation, in medical practice, it is considered 50% decrease of power density to a value in a depth of 1 cm below the surface.

The calculation formula of the effective penetration depth *d* is [1]:

$$d = \frac{1}{\sqrt{\pi f \mu \sigma}} \qquad (4.\ 11)$$

Where σ is electrical conductivity of the tissue, μ is permeability and *f* is frequency.

This expression is common electro-technical definition, it is a distance, where the intensity of electric field *E* decreases e-times against the value of the surface (e = 2,718).

5 Calculation, design, simulation and implementation of a planar applicator

In this chapter I will describe how to calculate length of waves, which are distributed in applicator. Then, I will show the process of design of applicator and my results of simulation in environment of program SEMCAD. I will present arguments why this model of applicator is the best. Finally, I will describe the process of the production of the applicator.

5.1 Theoretical calculations

In order to correctly determine the dimension of future applicator, I had to first calculate the length of the wave which is propagated in applicator. Wavelength in substrate about same permittivity and same permeability is calculated from following relation [1], [7]:

$$\lambda = \frac{\lambda_0}{\sqrt{\varepsilon_r \mu_r}} \tag{5. 1}$$

Where λ_0 is wavelength in vacuum, ε_r - is relative permittivity of substrate and μ_r –is relative permeability of substrate.

For wavelength in vacuum we know that it applies:

$$\lambda_0 = \frac{c}{f} \tag{5. 2}$$

where *c* is speed of light and *f* is working frequency.

If we apply equation (5. 2) on equation (5. 1) and, assuming that relative permeability μ_r equals one ($\mu_r = 1$), we obtain the relation for wavelength in future substrate:

$$\lambda = \frac{c}{f\sqrt{\varepsilon_r}} \tag{5. 3}$$

Because relative permittivity of applicator's substrate is different from the permittivity of the material into which the wave is propagated, we have to calculate with both of these values. We have to take into consideration the total relative permittivity, as arithmetic average of these two values. Moreover the situation is complicated by the structure of environment in which the wave is propagated. The applicator is in contact with the water bolus of 2 cm thickness and behind this water layer is irradiated tissue [8]. Relative permittivity of water and of tissue are also very different, therefore also here we take in consideration their arithmetic average. Total relative permittivity was calculated by relation:

$$\varepsilon_r = \frac{\varepsilon_d + \frac{\varepsilon_t + \varepsilon_v}{2}}{2} \tag{5. 4}$$

where ε_r is total ("effective") relative permittivity, ε_d is permittivity of dielectric substrate, ε_t is permittivity of tissue and ε_v is permittivity of water.

Substituting the values of different permittivities (for tissue (agar) 54, for water 81 and for substrate 4 (normally is in interval 4 – 5, 5)) into equation (5. 4), the result is:

$$\varepsilon_r = \frac{\varepsilon_d + \frac{\varepsilon_t + \varepsilon_v}{2}}{2} = \frac{4 + \frac{54 + 81}{2}}{2} = 35{,}75$$

Now when we know total relative permittivity, we can calculate length of wave propagates in applicator from relation (5. 3):

$$\lambda = \frac{c}{f\sqrt{\varepsilon_r}} = \frac{3 \cdot 10^8}{434 \cdot 10^6\sqrt{35{,}75}} = 0{,}1156\ m \ \rightarrow \ \lambda = 11{,}56\ cm$$

Wavelength in this applicator with these parameters is 11, 56 cm.

5.1.1 Calculation of dimensions of the applicator

In the bachelor I calculated the dimensions of applicator in a more simple way, because form of slot was a regular rectangle. Therefore, the result of wavelength could be only divided by 4. Now in the master thesis, the form of slot of applicator is sector of a circle, the most important dimension in this case is radius of circle *r* and I know that wavelength has to be equal to double radius plus a quarter circumference of a circle, as we can see from following relations.

Circumference of a circle O we can calculate simply as:

$$O = 2 \cdot \pi \cdot r \tag{5. 5}$$

Where r is radius of circle.

Furthermore, we know that it must apply:

$$11{,}56 = 2 \cdot r + \frac{2 \cdot \pi \cdot r}{4}$$

$$r = \frac{4 \cdot 11{,}56}{8 + 2 \cdot \pi}$$

Than radius r is:

$$r = 3{,}238\ cm$$

5.2 Influence of voxels size and shape of slot on the results

In the bachelor thesis I did not have proper conditions for simulation of applicator, because I could use only limited version of SEMCAD. In this version, number of voxels, which it was possible to make, was limited to one million cells. Now, in full version of SEMCAD X there is no limit of number of cells or this limit is very high.

As full version of SEMCAD X is now available, I am going to demonstrate how important the number of voxels is and why, then I would like to demonstrate the influence of the shape of the slot on the results.

5.2.1 Influence of number of voxels

Size of voxels in SEMCAD environment has significant impact of results. The reason of this fact is very simple. We create same structure with same parameters and same dimensions in SEMCAD and then we make voxels. If we use too big voxels can became that the voxels are bigger then structure or the voxels in model are at the interface of two structures with different characteristics, then SEMCAD calculates with parameters of structure, which has higher priority [15].

In my bachelor thesis I used bigger voxels, because I could not use smaller voxels due to the used limited version of SEMCAD. It meant that for example at the interface of metal layer, because this layer is very thin, and structure of water bolus on one side and structure of dielectric substrate on the other side, these voxels were filled with two different structures. Subsequently for the calculation and simulation results SEMCAD calculated in these voxels with parameters of structure with higher priority. Because metal layer has higher priority for calculation than water or dielectric substrate, SAMCAD calculated with these voxels as voxels full of metal and consequently the metal layer appeared to be thicker than in reality.

In the following picture (Picture 5-1) we can see the impact of different number of voxels on results of coefficient of reflection S_{11}. Blue line is result from my bachelor thesis, peak (minimum value) of this coefficient is exactly on position of frequency 434 MHz, it was the purpose and attenuation value is -9,5 dB. But if we use smaller, more detailed and precise voxels, we can see that the result is completely different – (see the red line) this coefficient achieves better value of S_{11}, attenuation value around -38 dB, but on the completely wrong frequency, somewhere around 586 MHz.

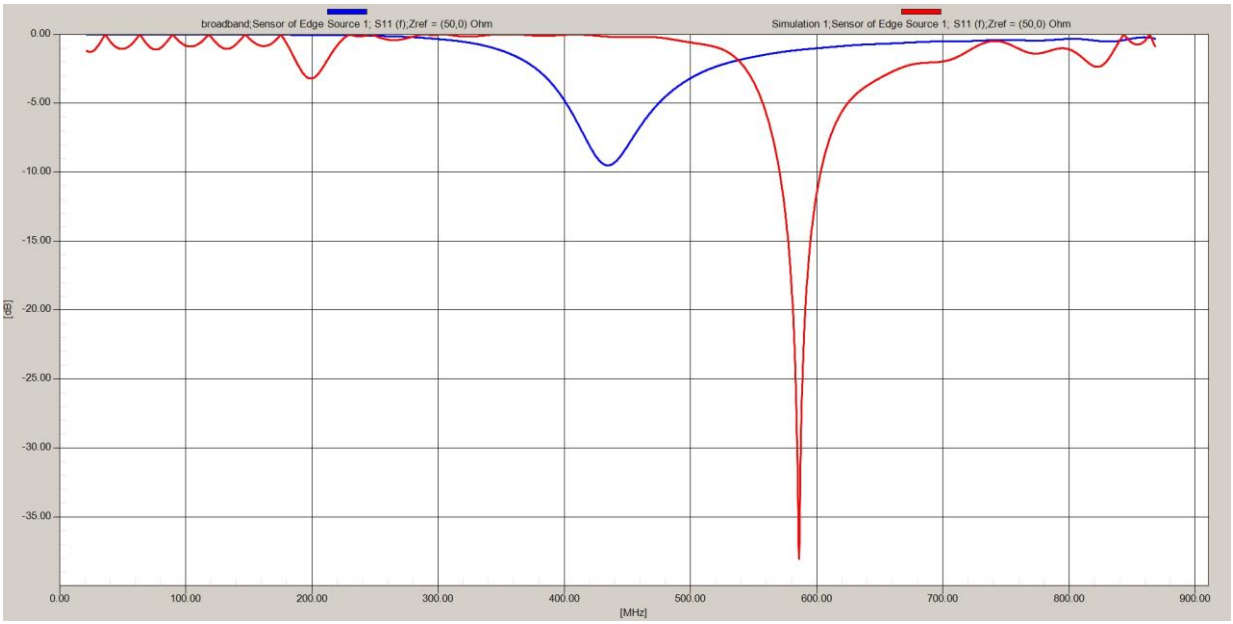

Picture 5-1 Impact of size of voxels on the results, blue line – bigger voxels in bachelor thesis, red line - more detailed and precise voxels in master thesis.

Such significant alternations of results of reflection coefficient S_{11} also had impact on result of distribution of SAR - specific absorption rate. In the following pictures (Picture 5-2) and (Picture 5-3) we can see distribution of SAR firstly for applicator with lower number of voxels, thus result from bachelor thesis and then result for the same applicator but with more precise calculation. Both of them represent the SAR at the surface of the skin.

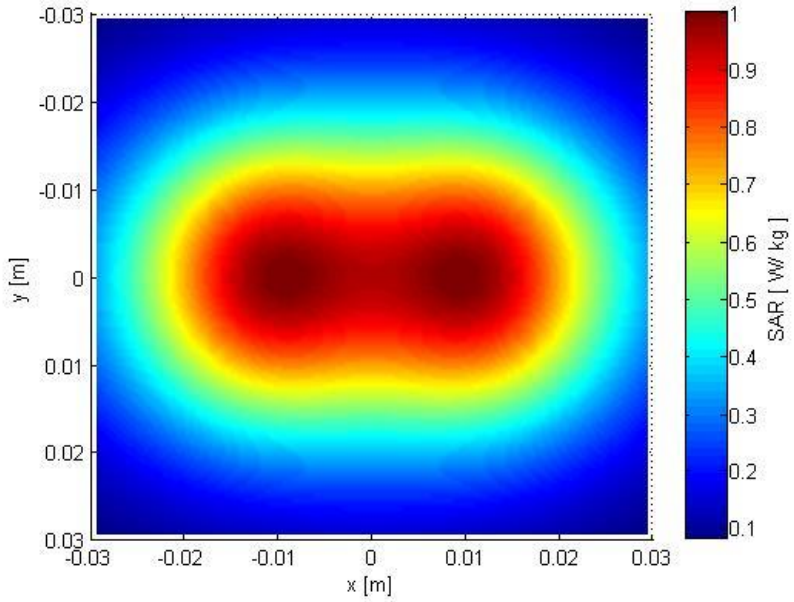

Picture 5-2 Specific absorption rate by lower number of voxels, result from bachelor thesis.

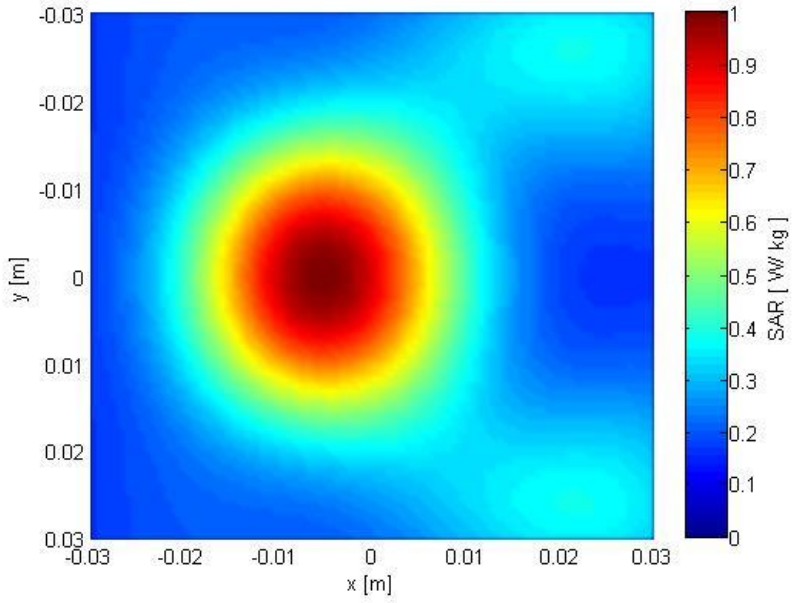

Picture 5-3 Specific absorption rate with more detailed and precise voxels.

In this case, I decided not to compare the effective penetration depths, because from the above mentioned facts it is evident that the results obtained in the bachelor thesis were substantially imprecise, and it serves as an illustration how important the setting of voxels is.

All the following results were obtained with more detailed and precise voxels.

5.2.2 Influence of shape of slot on the results

In this small chapter I want compare tow models which have only one difference and that is the shape of the slot.

I will compare the model mentioned above and the model with the shape of sector of circles, as it should be in the case of one quadrant of the master thesis. We can see both of them in the picture (Picture 5-4) below. Dimensions of both applicators are the same. You can see them in the following table (Table 1).

Structure	Dimension (mm)
axis length of slot	115,6
width of gap	0,5
side of the outer square	60
plating thickness	0,03
Thickness of substrate	1,5

Table 1 Dimensions of the applicators.

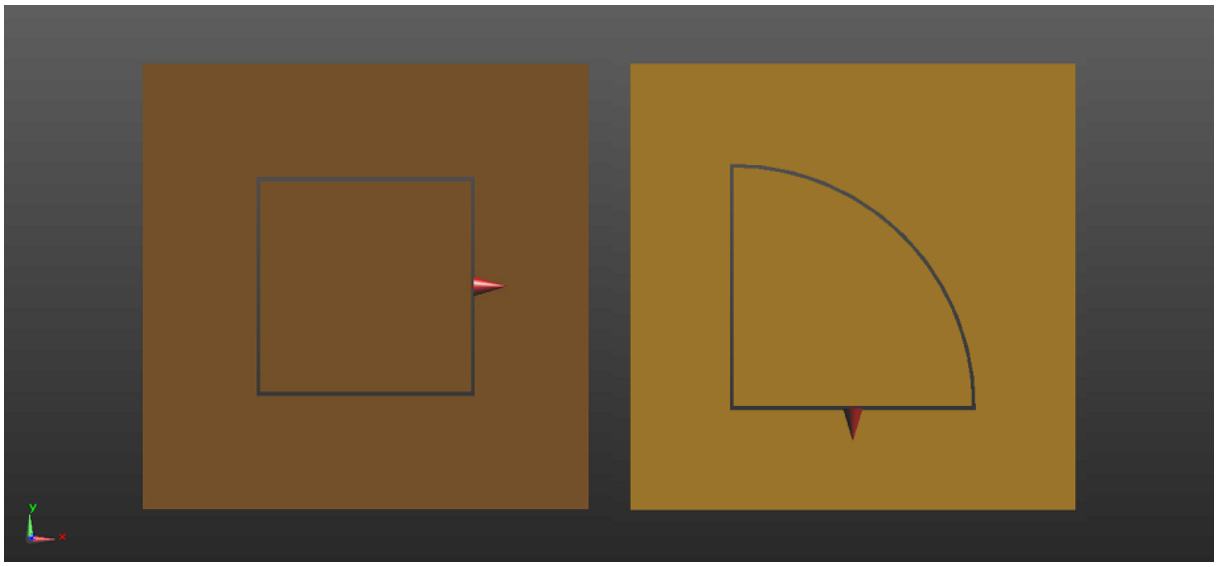

Picture 5-4 On the left is shape of slot from bachelor thesis, on the right is shape of slot from master thesis.

In bachelor thesis I used two sources on the opposite sides of the square and exactly in the middle of square's side, but for the purpose of comparison of two different shape of slot I used only one of them, because logically the results with one and two sources have to be different.

Just like in the first case, we can see difference between results of coefficient of reflection S_{11} in the picture (Picture 5-5) below.

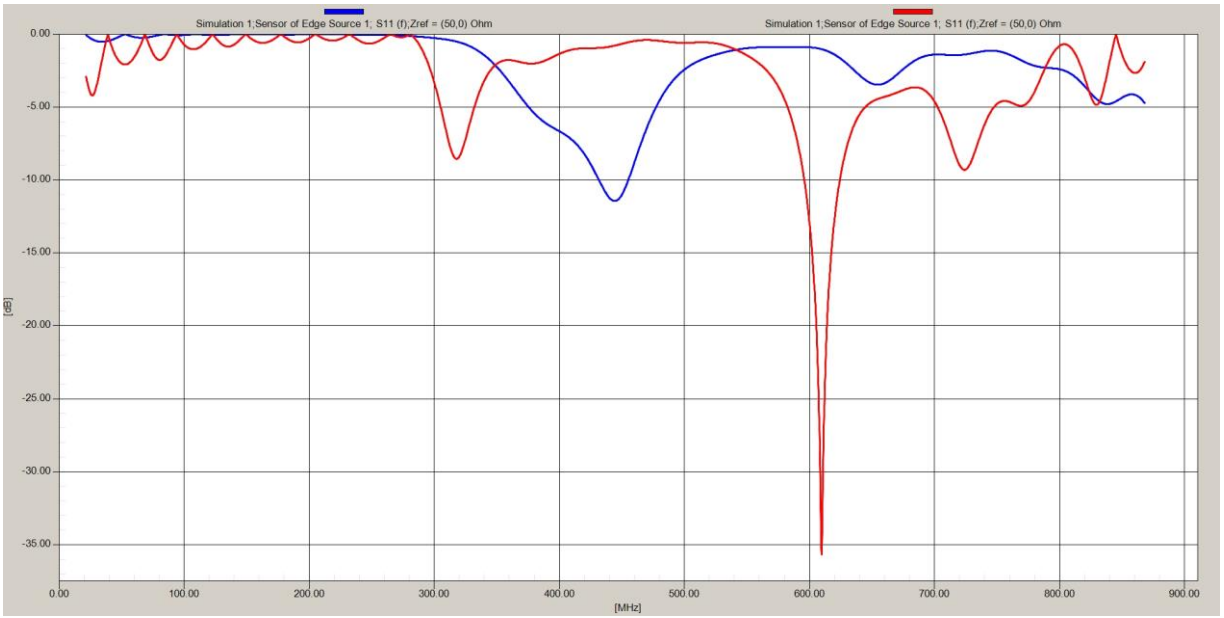

Picture 5-5 Impact of shape of slot on the results, blue line – square slot, red line – sector of circle slot.

Blue line represents coefficient S_{11} of model with square slot, it is evident that this peak is smaller than the other shown by the red line. His minimum is on frequency 445 MHz where it has value of -11,4 dB, on the desired frequency 434 MHz the value is -10,3 dB. The red line represents coefficient S_{11} of model using a sector of circle slot. The peak of coefficient S_{11} is very deep, more than -35 dB, but his position is on frequency around 610 MHz, so we can see, that applicator with sector of circle slot does not have good impedance matching at the operating frequency 434 MHz.

Also distribution of SAR will be different for both of types of slot, as we can compare from the following pictures of distribution of specific absorption rate. As first, it shows SAR in case of square slot (Picture 5-6), then in case of sector of circle slot (Picture 5-7).

For completeness, I also mention the distribution of SAR in depth 1 cm below the surface of the skin, where the SAR is considered to be the maximum, thus 100 %.

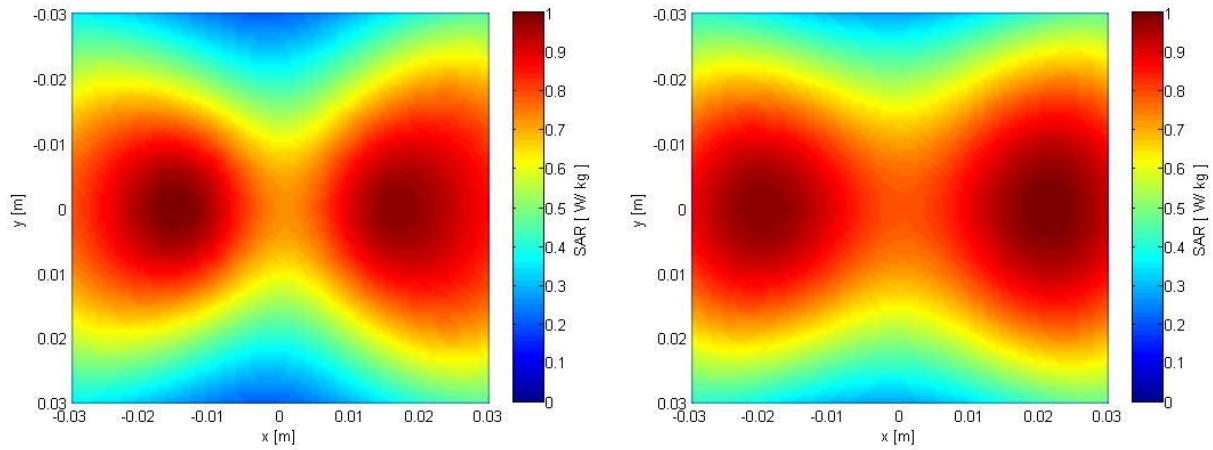

Picture 5-6 a) (left) SAR - Specific absorption rate of model with slot of shape regular square on the surface of the skin and b) (right) in depth 1 cm below the surface of skin.

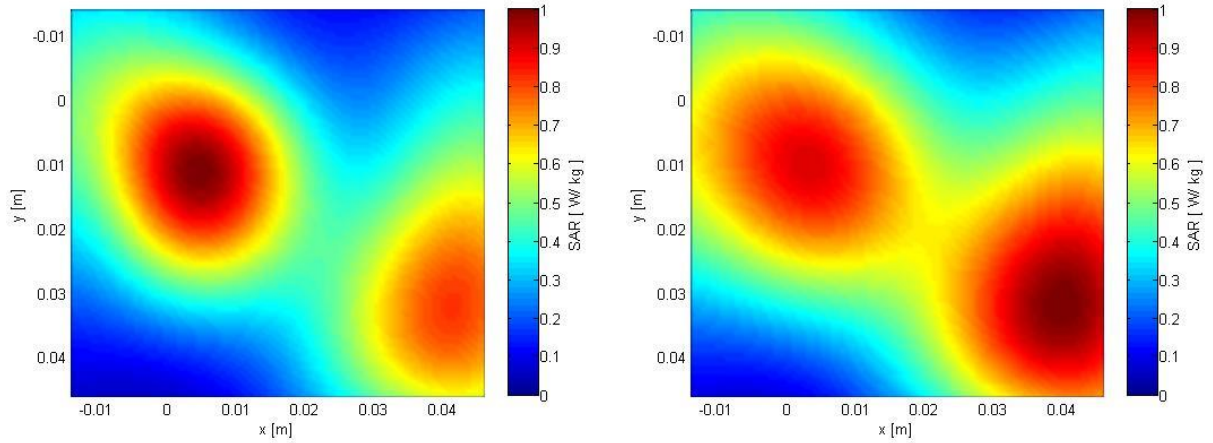

Picture 5-7 a) (left) SAR - Specific absorption rate of model with slot of shape sector of circle on the surface of the skin and b) (right) in depth 1 cm below the surface of skin.

In the previous figures we can see, that distribution of specific absorption rate is also influenced by the shape of the slot. In both cases there were two focuses of radiation. In the case of square shape the focuses were originated exactly opposite from each other at the point of excitation. In the other case, first focus was on the right side, but not in the point of excitation and the other was in the curved part of the slot. In the second case the focuses were farther from each other than in case of a square gap. Also pictures of specific absorption rate in depth 1 cm below the surface of skin look different, it seems that in case of a square slot the SAR is higher, but we see this better from effective penetration depth.

Effective penetration depth is a parameter which we can calculate as 50% decrease of value SAR in 1 cm below the surface of skin, because here the value of SAR is 100 %. You can see in the following figures the SAR calculated using the SEMCAD and next contours of 50 % and 25 % of value of the SAR calculated using the MATLAB. I viewed the effective penetration depth in both axes, Y (Picture 5-8 a) and b)) and X (Picture 5-9 a) and b)).

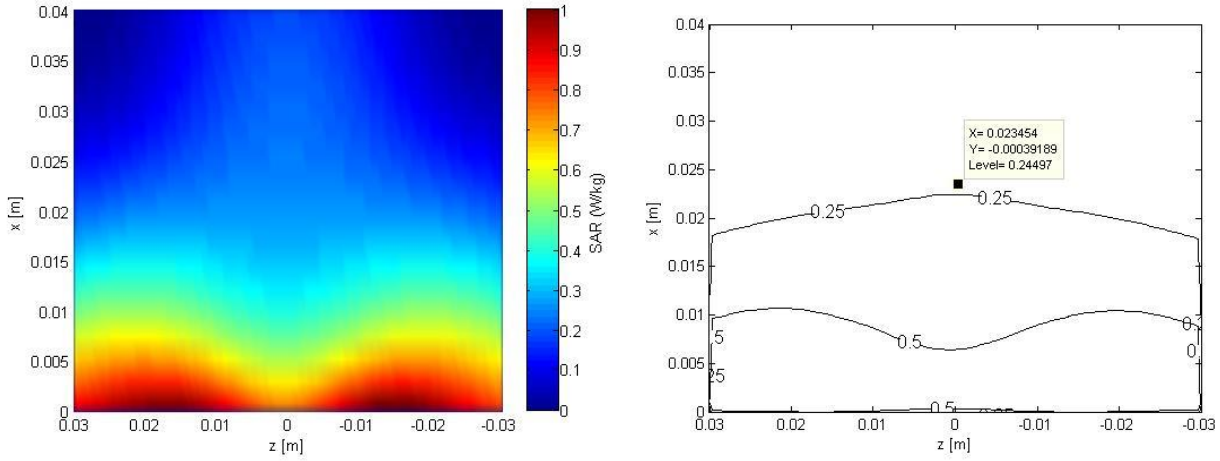

Picture 5-8 Effective penetration depth of square slot – axis Y a) slice in axis Y, b) contours of 50 % and 25 % of value of SAR.

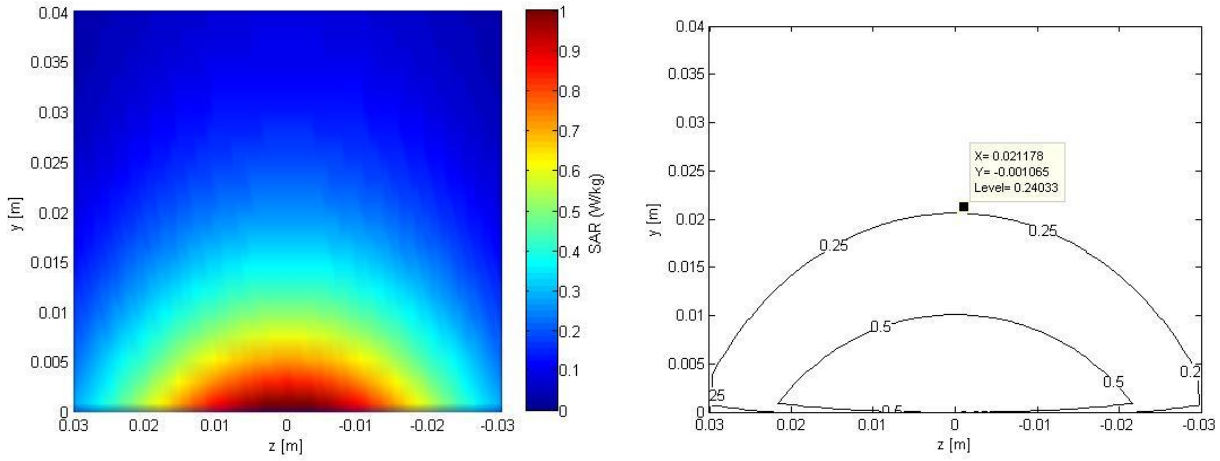

Picture 5-9 Effective penetration depth of square slot – axis X a) slice in axis X, b) contours of 50 % and 25 % of value of SAR.

We can see, that in the picture of axis X (Picture 5-9) it was showed only one focus and in the other figure (Picture 5-8) of axis Y were manifested both of focuses. It corresponds with figure of distribution of specific absorption rate SAR of model using slot of regular square shape. Effective penetration depth is more than 2 cm below the surface of skin in both cases of slices.

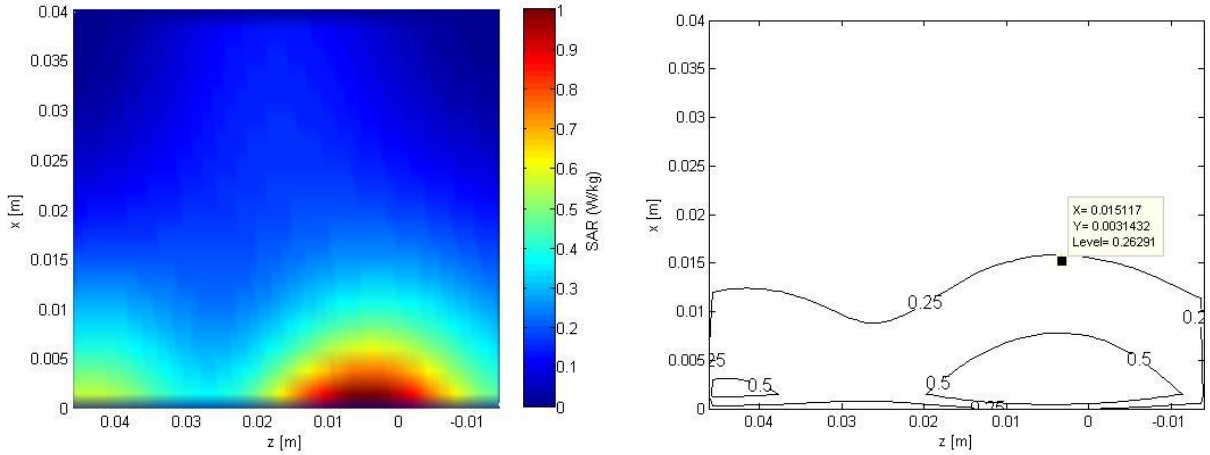

Picture 5-10 Effective penetration depth of sector of circle slot – axis Y a) slice in axis Y, b) contours of 50 % and 25 % of value of SAR.

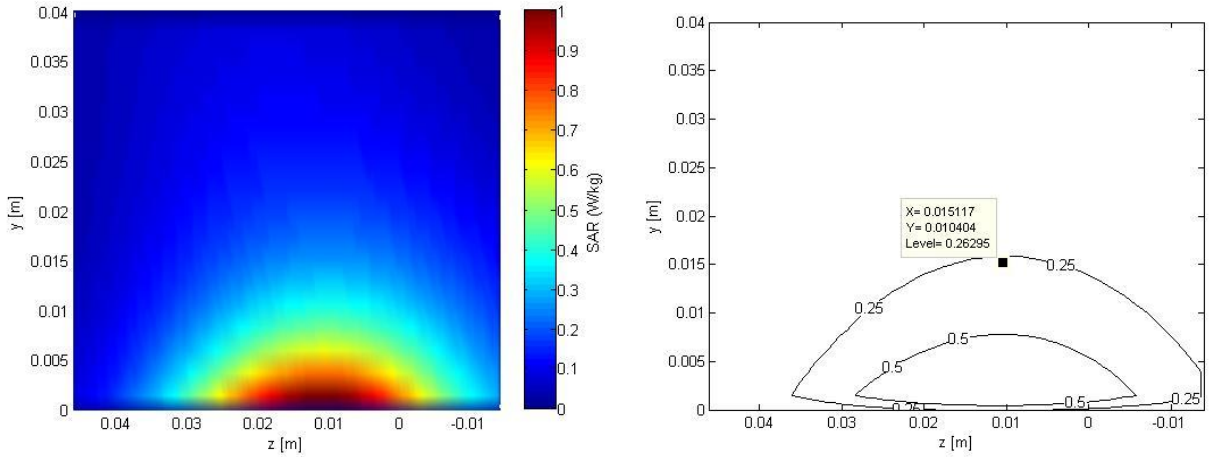

Picture 5-11 Effective penetration depth of sector of circle slot – axis X a) slice in axis X, b) contours of 50 % and 25 % of value of SAR.

As in the previous example pictures (Picture 5-10) and (Picture 5-11), of model using sector of circle slot shape, of the X axis, we can see only one focus. When we display it in the Y axis, we can see two focuses, as we can observe in the figure of distribution of specific absorption rate SAR of model with sector of circle slot. Effective penetration depth is little bit less than in previous case, it is about 1,5 cm below the surface of skin in both cases of slices.

5.2.3 The conclusions

In the case of the square shape we can say that impedance matching is satisfactory, minimum of coefficient S_{11} is very close to the desired operating frequency of 434 MHz and on this frequency reaches values -10,3 dB, what is representing more than 90 % of the transferred power. The focuses are in case of the square closer together, so the distribution of SAR is more homogeneous. The effective penetration depth is higher, about approximately 7 millimeters.

In the case of the circular sector slot, the minimum of coefficient S_{11} is very significant, but on the completely wrong frequency and on the desired operating frequency of 434 MHz its value is close to zero. As regards the distribution of SAR, result of this applicator is more inhomogeneous and values of absorbed power are less than by square slot.

Considering all the results in this chapter, it is clear, that the size and number of voxel, as well as the shape of the slots have a significant impact on the behavior of the applicator. Differences were reflected in both cases in all parameters. Impact of shape of the slot of effective penetration depth is also important. In the case of the square shape the value of effective penetration depth achieved more than 2 cm whereas in the case of the circular sector shape the value achieved only 1,5 cm.

After summary of all the conclusions, we can say that applicator with these dimensions and parameters, is more effective when using the slot in shape of a regular square.

5.3 Optimization of one quadrant of applicator in SEMCAD

The task of my master thesis was not primarily focused on optimization of quadrant of applicator, but design entire matrix from four the same quadrants. But as a first logical step was design one functional quadrant. Assumption was that if works one quadrant, then fine tuning of the whole matrix of quadrants will be easier.

The shape of the slot in my work (sectored circle) was proposed by my supervisor sector of circle, as you can see in the picture from SEMCAD below (Picture 5-13).

Based on my experience from my bachelor thesis I knew that the most important parameter is wavelength. I calculated it in the same way as before thanks to the knowledge of permittivities of all structures and working frequency, 434 MHz. This wavelength, 11,56 cm, determined the size of inner metalized part of the applicator which also has a shape circle's sector. For the most correct functioning of the applicator on frequency 434 MHz, the length of wavelength had to be exactly in the middle of the slot [1], [16]. For better understanding, please see the picture below (Picture 5-12). All calculations can be found in subchapter "Theoretical calculations". I chose the width of the slot 1 mm, so two times wider than in bachelor thesis, because in the curved part of slit there were inaccuracies in plotting of model in SEMCAD.

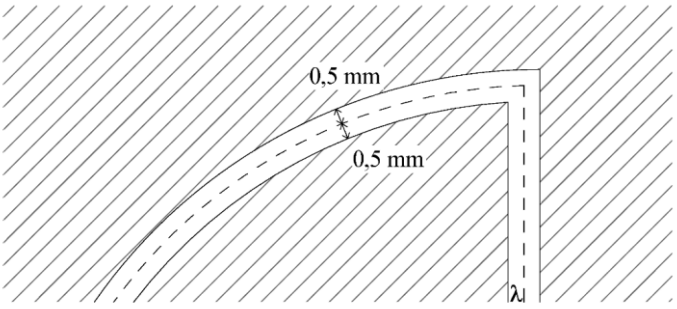

Picture 5-12 Drawing of position of wavelength in the middle of slot.

I optimized the model by changing the size of the outer edges of the square, or ground. I observed that with increase of the size of edges, the working frequency decreases, because the impedance increases. This mechanism works logically also vice versa. I achieved the best results when the size of the outer edges of the square was 71 mm.

I also tried to change the position of the slot and inner metalized part of the applicator from the center to the sides. I received the final model thanks displacement of the slot about 1 mm to the left from the center of model. The resulting dimensions of the applicator are shown in table (Table 2) below.

Structure	**dimension (mm)**
the length of the central axis of the slot	115,60
width of gap	1,00
side of the outer square	71,00
plating thickness	0,03
thickness of substrate	1,50
radius of inner metalized circle's sector	32,13

Table 2 Dimensions of the applicator.

The applicator is excited by a single source located exactly in the middle of one of the straight parts of the circle's sector. Coaxial power supply connects both metalized parts of the applicator such that the inner conductor is soldered to the inner part and the outer conductor to the outer part. The inner conductor of the coaxial cable is powered 1,5 mm from the edge of the inner metalized part of applicator.

The values of parameters used for the simulation of applicator and the specified in program SEMCAD are summarized in the following table (Table 3) below.

material	relative permittivity ε	conductivity σ (S/m)	density ρ (kg/m^3)
dielectric substrate (kuprextit)	4	-	-
biological tissue	54	0,8	1050
distilled water (bolus)	81	-	1000

Table 3 Values of parameters used for the simulation [17].

In a simulator SEMCAD I created a three-dimensional model (Picture 5-13) and to each structure I assigned features and parameters mentioned above.

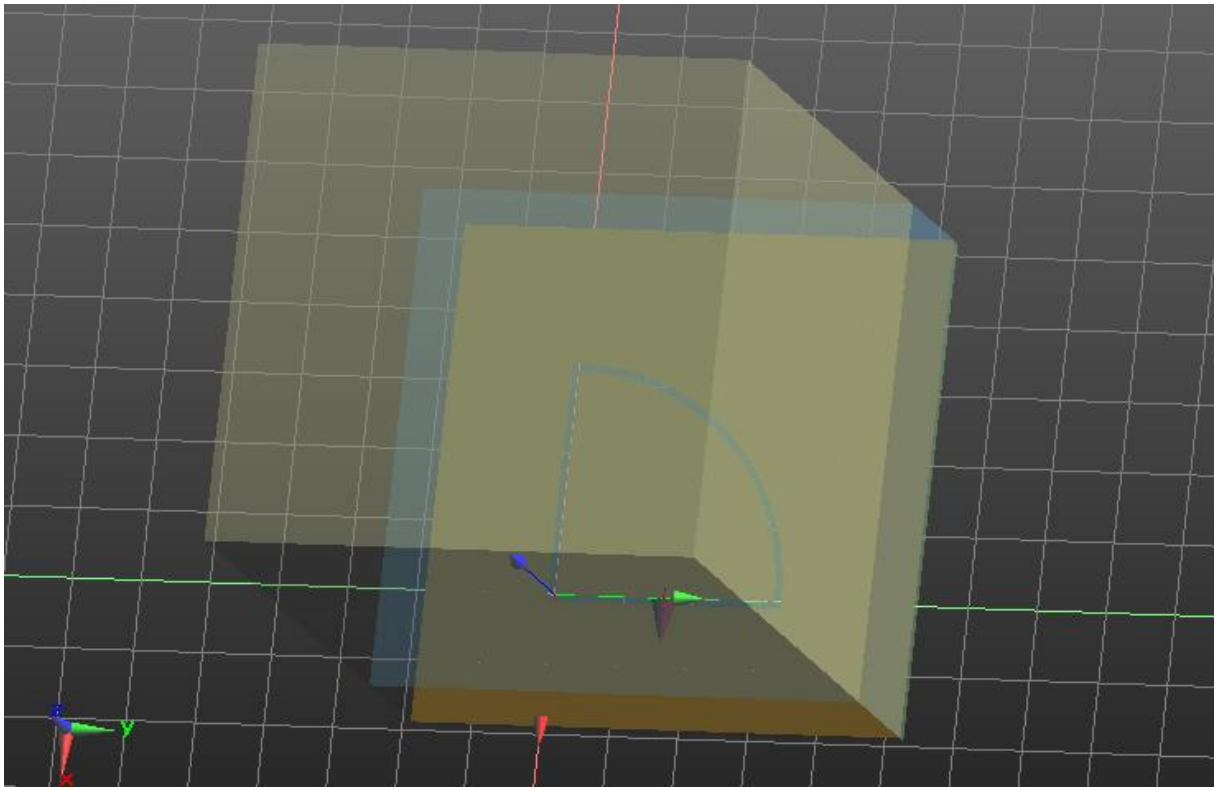

Picture 5-13 Model in an environment of simulator SEMCAD

5.3.1 Coefficient of reflection S_{11}

In the graph (Picture 5-14) of coefficient S_{11} we can see, that minimum of S_{11} is located very near of the desired operating frequency, exactly of frequency 423,5 MHz where it reaches a value of attenuation -14,55 dB. However, on frequency 434 MHz it reaches a value of attenuation -13,15 dB. As I mentioned, at attenuation -10 dB the value of transferred power is around 90 % and only 10 % is reflected back [15]. This result is considered adequate and sufficient. In the graph we can see also harmonic wave, which is manifested with other attenuation on frequency around 860 MHz, thus near the harmonic frequency of 868 MHz, but attenuation is weaker, -12,5 dB.

In conclusion, we can say that this resonant circuit is sufficiently impedance matching at the frequency of 434 MHz. Value of the ratio of standing waves achieved 1,57, thus less than 2 as it was specified in the work assignment.

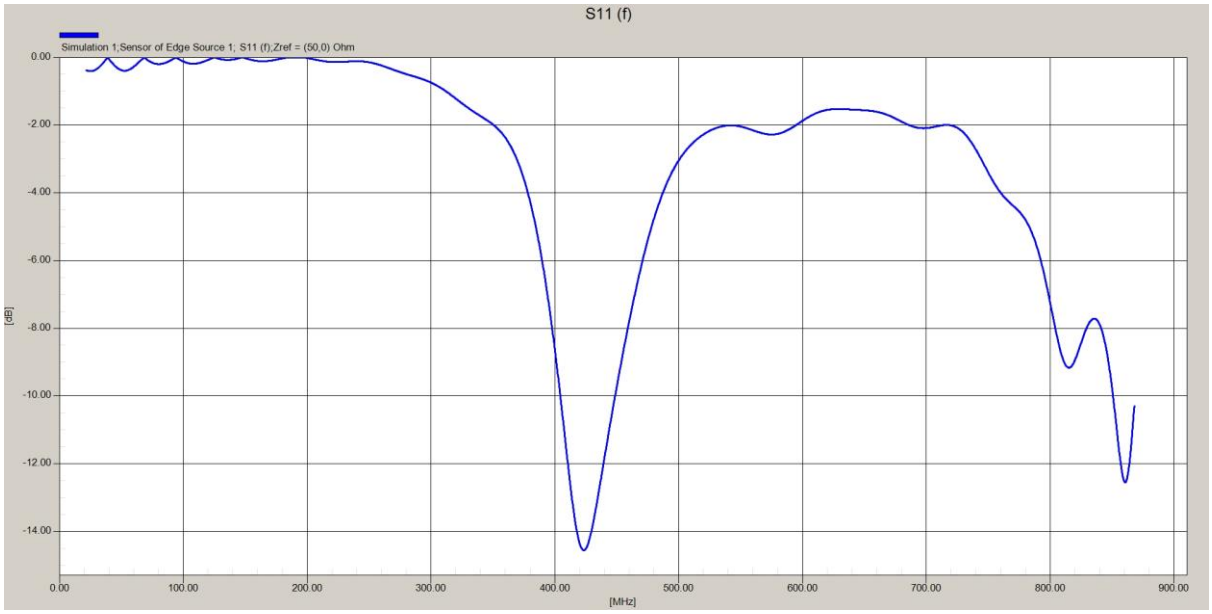

Picture 5-14 Frequency response of coefficient of reflection S_{11}, the value on desired operating frequency 434 MHz is -13,15 dB.

5.3.2 Effective aperture – distribution of specific absorption rate - SAR

In the picture below (Picture 5-15 a)) we can see distribution of specific absorption rate on the surface of skin, the area of penetration is not exactly round, but it is homogenous with one focus in the middle of effective aperture. By using the Adobe Illustrator I drew the shape of slot as a black line for better imaging the focus is formed depending on the position of the slot.

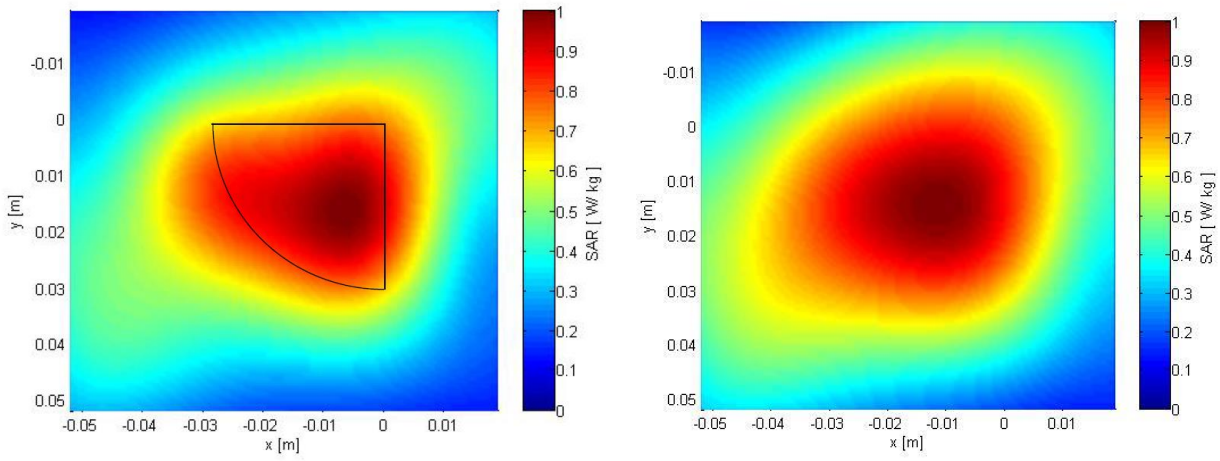

Picture 5-15 a) (left) Specific absorption rate on the surface of skin and b) (right) , 1 cm under the surface of skin.

In the other figure (Picture 5-15 b)) we can see distribution of specific absorption rate SAR in 1 cm under the surface of skin, here the value of SAR is considered 100 % of value of SAR, in place of decline in the value by 50% is the effective penetration depth, will be shown later.

5.3.3 Effective penetration depth

Theoretical description of effective penetration depth can be found in subchapter "parameters defining conduction". In the following pictures (Picture 5-16 a)) and (Picture 5-17 a)) you can see by SEMCAD calculated distribution of SAR in agar along axis Y and axis X. In the pictures (Picture 5-16 b)) and (Picture 5-17 b)) you can see contours of 50 % and 25 % of value of SAR calculated by MATLAB. In both cases the value of the effective penetration depth achieves more than 2,4 cm.

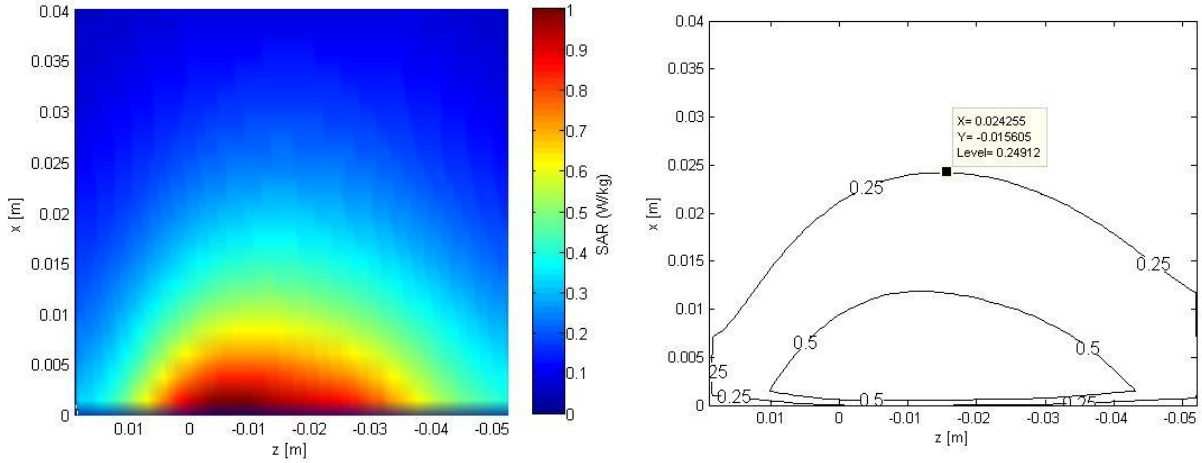

Picture 5-16 Effective penetration depth of one quadrant – axis Y a) slice in axis Y, b) contours of 50 % and 25 % of value of SAR.

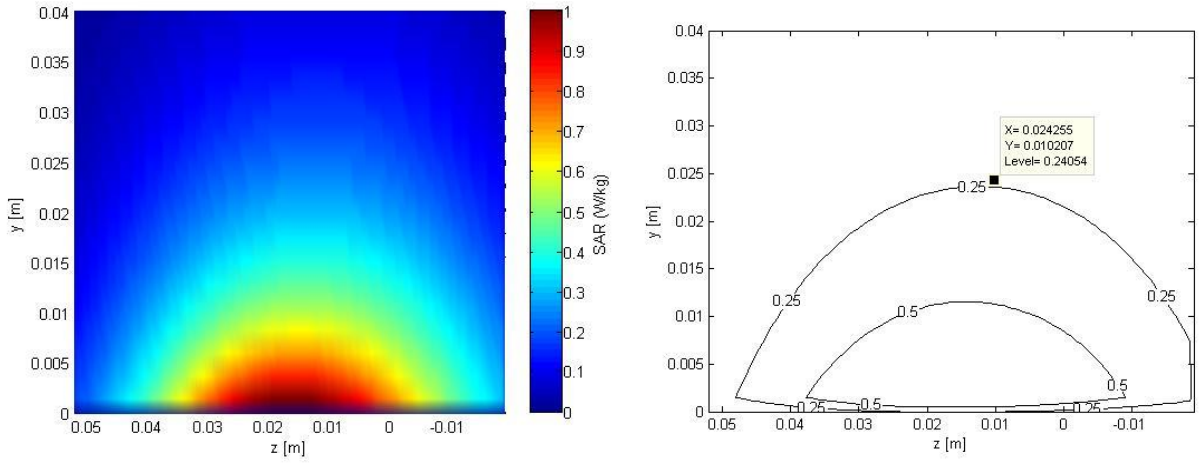

Picture 5-17 Effective penetration depth of one quadrant – axis X a) slice in axis X, b) contours of 50 % and 25 % of value of SAR.

In the last picture (Picture 5-18) of this model we can see distribution of SAR in effective penetration depth, thus in depth which corresponds with decline in value by 50 % from value in depth 1 cm under the surface of skin. Value of effective penetration depth in this case is 2,4 cm.

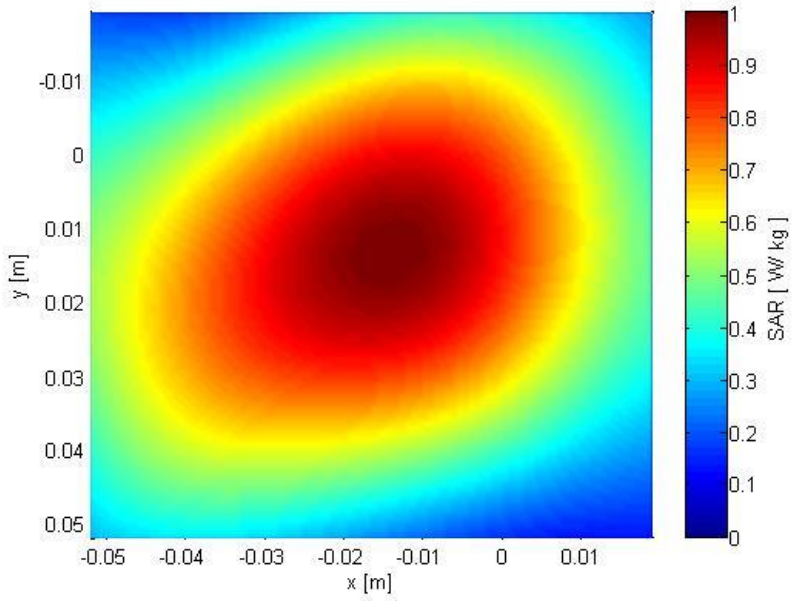

Picture 5-18 SAR - Specific absorption rate, 2,4 cm under the surface of skin in effective penetration depth with shape of slot.

After analysis of distribution of SAR and frequency response of coefficient of reflection S_{11}, we can say that this resonant circuit has sufficient impedance matching at the frequency of 434 MHz and its distribution of SAR is also satisfactory. Therefore, I decided to use this model for further processing and the formation of the resultant matrix applicator.

5.4 Design and simulation of the complete model of matrix of four quadrants in the SEMCAD

For design of the complete model of matrix of four quadrants I used model of one quadrant which I have presented above.

My progress of work was as follows. I pasted the same model four times into new project and by using rotation and translation I created final structure of applicator. I made the same also with sources, so finally on one half of structure, on two quadrants the sources were excited in inner structure of the slot and on the opposite side were exited in the outer side of the slot. The result was that the applicator worked only on the side with sources exited on the inner side of the slot and on the opposite side did not irradiate. After turning the resources so that all of them were excited in the inner metalized part of quadrants (the inner conductor of the coaxial cable was connected with this inner part of quadrant), the model started to work. The first result of the matrix can be seen.

At first, I was interested in how the compilation of matrix manifests on the frequency during of the coefficient of reflection S_{11}. In the chart below (Picture 5-19), where are shown curves of S_{11} of all four sources, it can be seen that frequency responses of all sources are identical. Minimum of S_{11} is on the frequency 427,5 MHz and achieves value -19,9 dB, on the desired operating frequency of 434 MHz achieves -17,35 dB.

Thus we can see, that the compilation of matrix had a positive impact on frequency, because the frequency was shifted closer to the desired operating frequency of 434 MHz from 423,5 MHz to 427,5 MHz, and the S_{11} on frequency 434 MHz decreased from -13,15 dB to -17,35 dB.

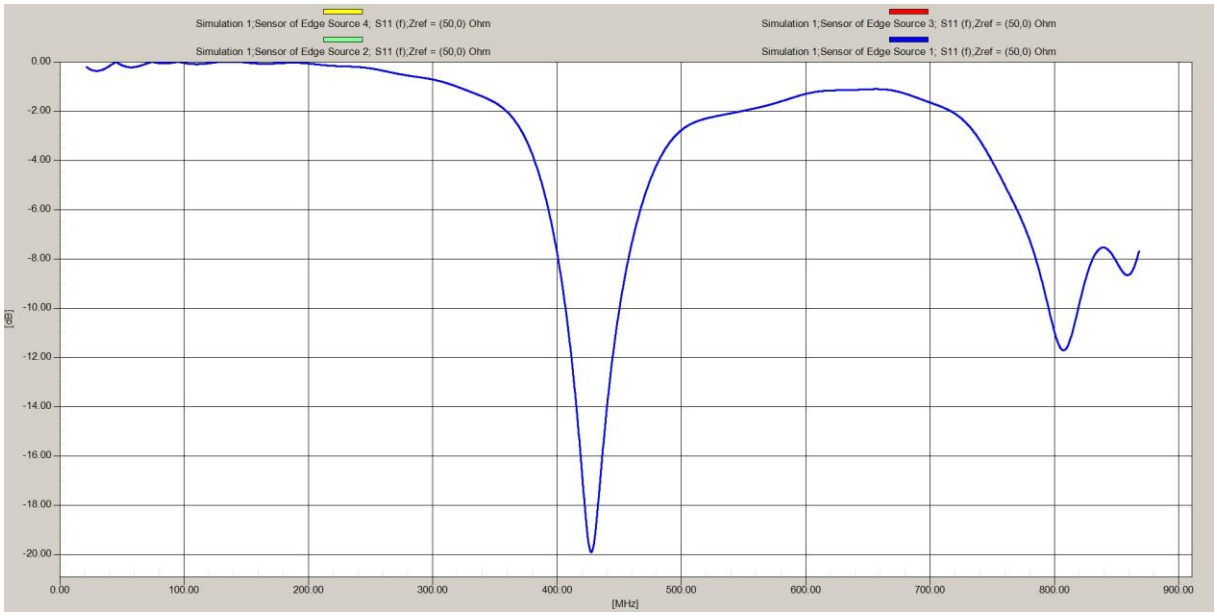

Picture 5-19 Frequency response of coefficient of reflection S_{11}, the value on desired operating frequency 434 MHz is -17,35 dB.

The other important parameter for the determination of proper functioning of the model is distribution of the SAR. In the following picture (Picture 5-20) we can see inhomogeneous distribution of the SAR forming a simple composition of quadrants in a square matrix. The slots are too far apart and therefore, four separate focuses of radiation were formed.

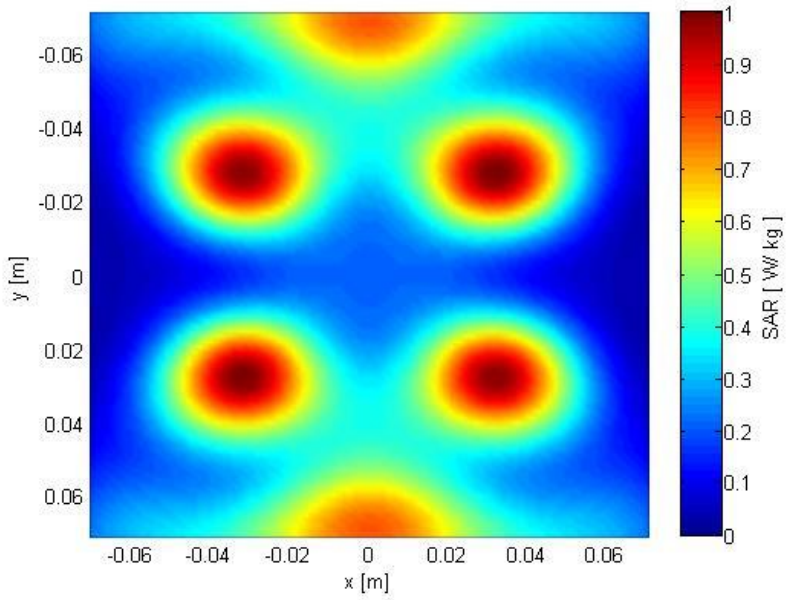

Picture 5-20 SAR - Specific absorption rate, on the surface of skin.

It is evident that this model with this distribution of the SAR is not suitable and that requires correction. Therefore I will not continue giving additional projection of this model.

Having analyzed the distribution of the SAR by last model, as the next logical step of adjustments consists of approximation of the slots closer together and thus reducing the cold spaces between the slots. I narrowed the gap between the slots along both axes by half, now the gap between slots is 17,62 mm. The results of this solution are shown in the graph (Picture 5-18) below.

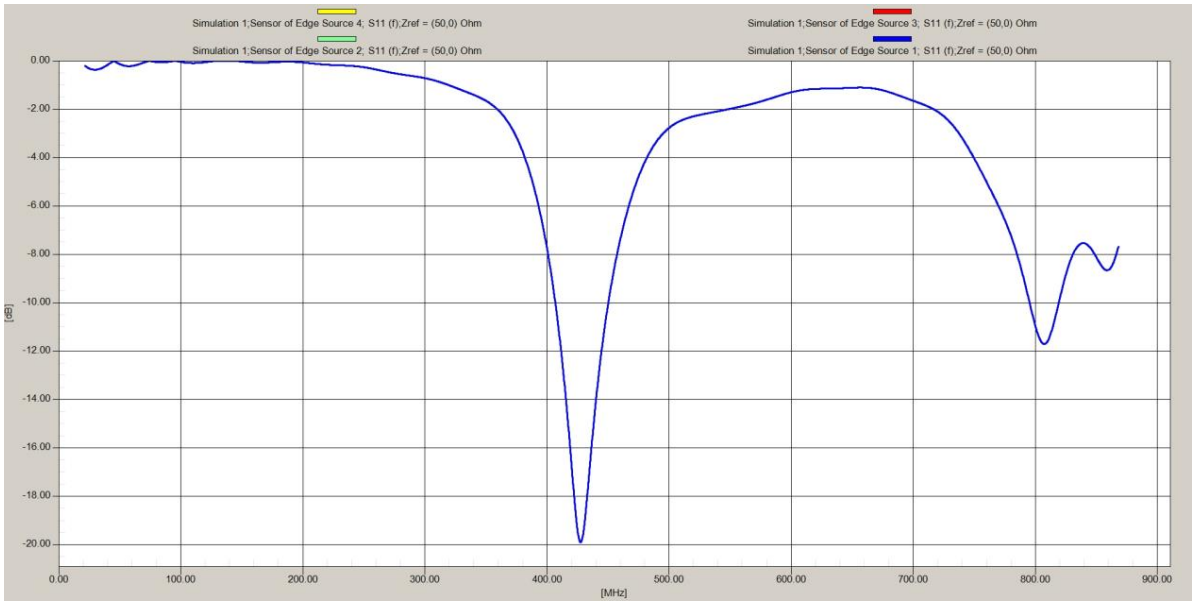

Picture 5-21 Frequency response of coefficient of reflection S_{11}, the value on desired operating frequency 434 MHz is -14,0 dB.

Approximation of the slots closer together had impact on frequency response S_{11}, but not much significant. In the chart above (Picture 5-21) you can see the result, it is still satisfactory, the minimum shifted to the frequency 420,5 MHz with value -20,9 dB, on the operating frequency 434 MHz the value was increased from -17,35 dB to -14 dB, which is very similar result like in case of one quadrant.

But even more interesting effect was reflected in the distribution of the SAR's values. As shown in the following figure (Picture 5-22), only two focuses appeared closer together, but still the area of radiation is not completely homogenous.

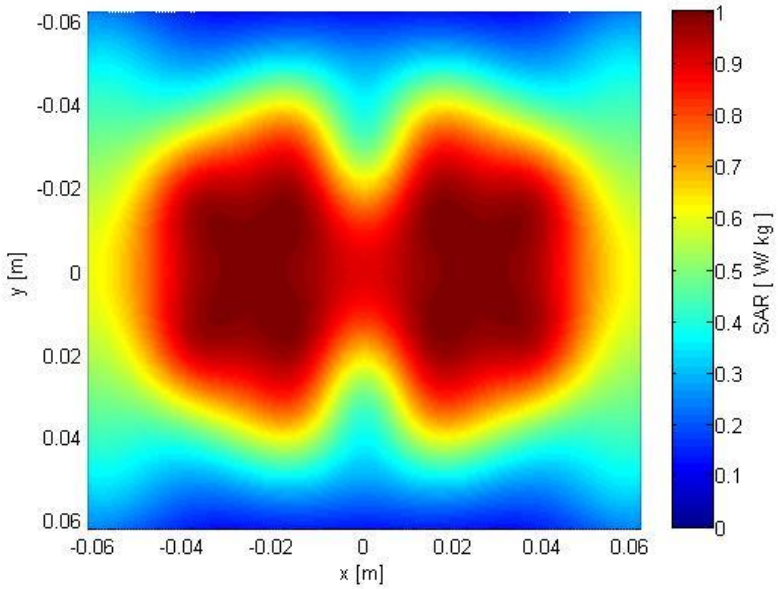

Picture 5-22 SAR - Specific absorption rate on the surface of skin.

From the previous developments in the distribution of the SAR and S_{11}, I decided to continue in approximation of the slots, but only along the Y axis, where the gap between focuses still exists, because the impact of these adjustments is not significant, considering the coefficient of reflection S_{11}.

As a further modification I moved the slots along axis X by further 8 mm. This means that the gap's width along axis X is 9,62 mm. You can see the results in the following picture (Picture 5-23).

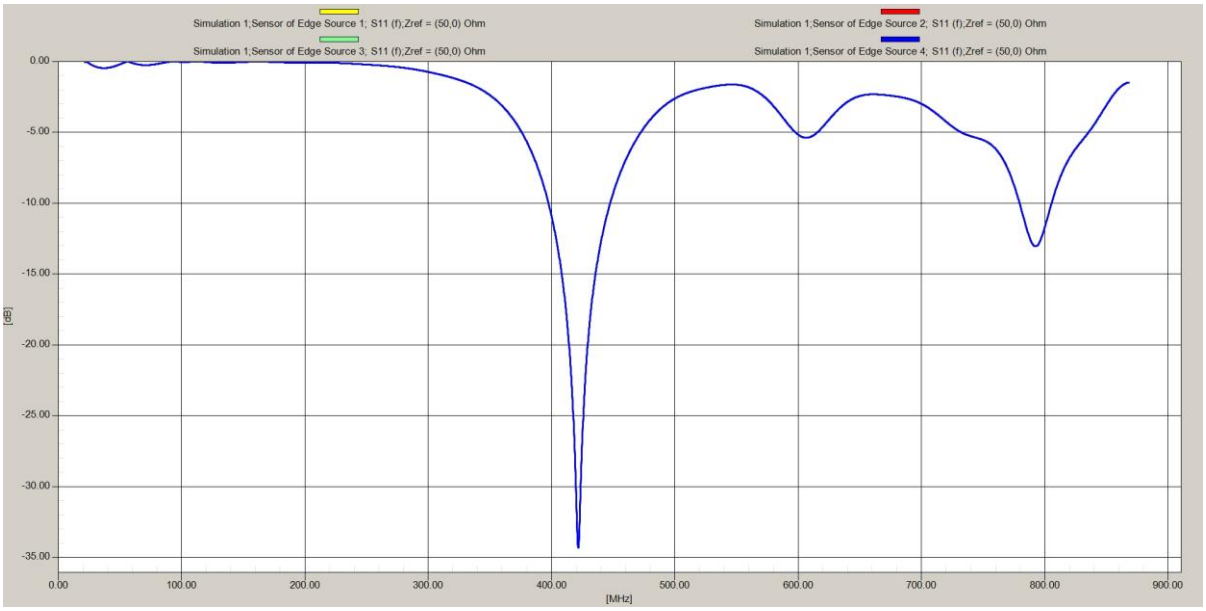

Picture 5-23 Frequency response of coefficient of reflection S_{11}, the value on desired operating frequency 434 MHz is -16,0 dB.

We can notice that in case of S_{11} no significant shift of frequency can be observed, as it still ranges between 420 – 423 MHz. Here the minimum is on frequency 421,6 MHz, but the value of decibels is significantly lower, -34,3 dB, to decrease over the previous model occurred also on our desired operating frequency of 434 MHz to -16,0 MHz.

Thus, as I mentioned before, more important parameter to select the best model will be the distribution of the SAR's values. The next figure of the SAR (Picture 5-24 a)) seems homogenous.

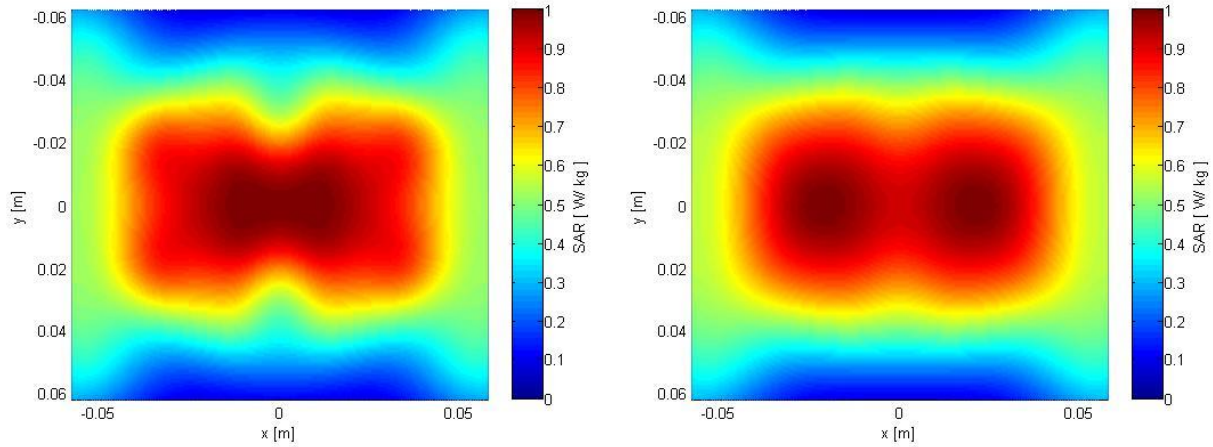

Picture 5-24 a) (left) Specific absorption rate on the surface of skin and b) (right) in 1 cm under the surface of skin

But when one takes a look at the next picture (Picture 5-24 b)) of the SAR in one centimeter below the skin, where the maximum of the SAR is concentrated, it is still possible distinguish the two focuses of radiation.

Therefore, I tried to narrow down the gap between slots along axis X again, by further 5 mm at just 4,62 mm. Results are shown again below in the graph (Picture 5-25). The peak near our desired operating frequency has minimum at frequency 430 MHz with the value -19,4 dB and at frequency 434 MHz it achieves value of decibels -18,5 dB.

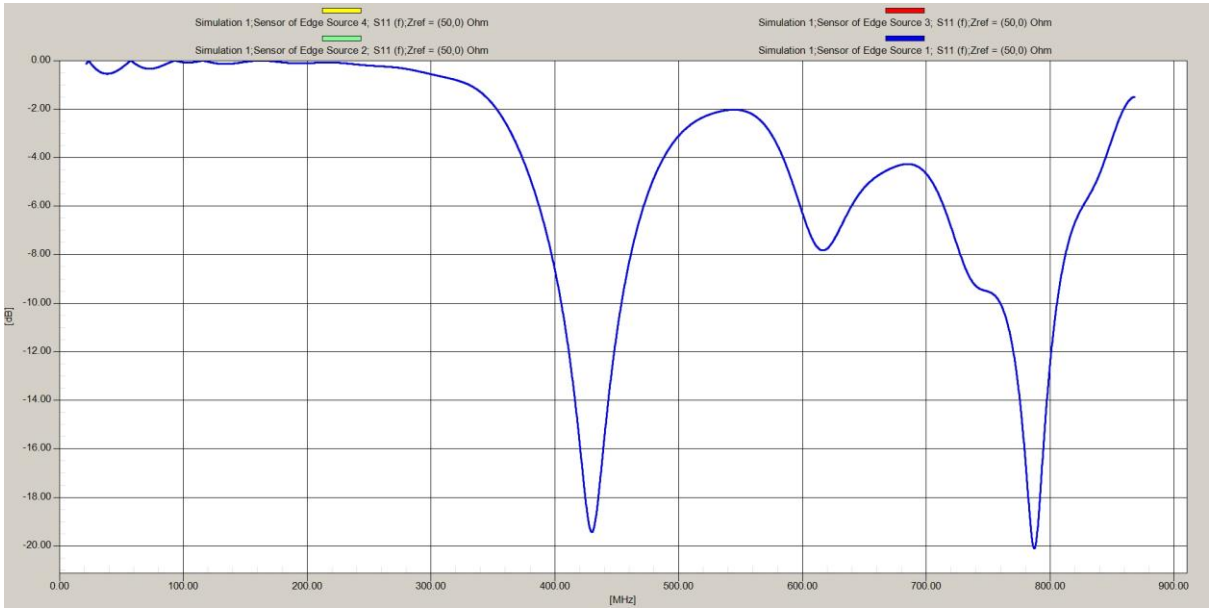

Picture 5-25 Frequency response of coefficient of reflection S_{11}, the value on desired operating frequency 434 MHz is -18,5 dB.

But as we can see in this case there were more significant harmonic waves. This fact would have significant impact on results during the measurement and could cause to disruption of the measurement results. What is more, there was also another wave, not only around frequency 800 MHz, but also around 600 MHz.

In the figures of distribution of specific absorption rate (Picture 5-26 a) and b)) it is obvious that area of radiation is homogenous in both cases, as on the skin surface but as well one centimeter under the skin.

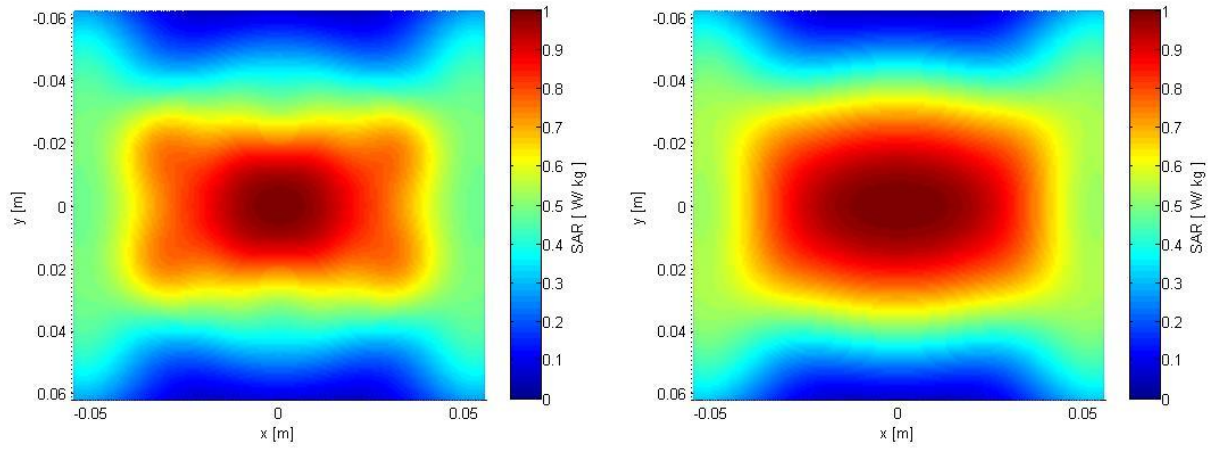

Picture 5-26 a) (left) Specific absorption rate on the surface of skin and b) (right) in the 1 cm under the surface of skin

But I found this model inconvenient due to the frequency during of coefficient of reflection S_{11} also.

Further I tried to find the optimal position of the slots and the optimal width of the gap between them so that the area of radiation would be homogenous and at the same time the harmonic wave would be not so much significant in the frequency during of S_{11}. I changed gradually the distance between the slots by 1 mm. I achieved the best results with width of the gap between the slots amounting to 6,62 mm, as you can see further in the picture (Picture 5-27).

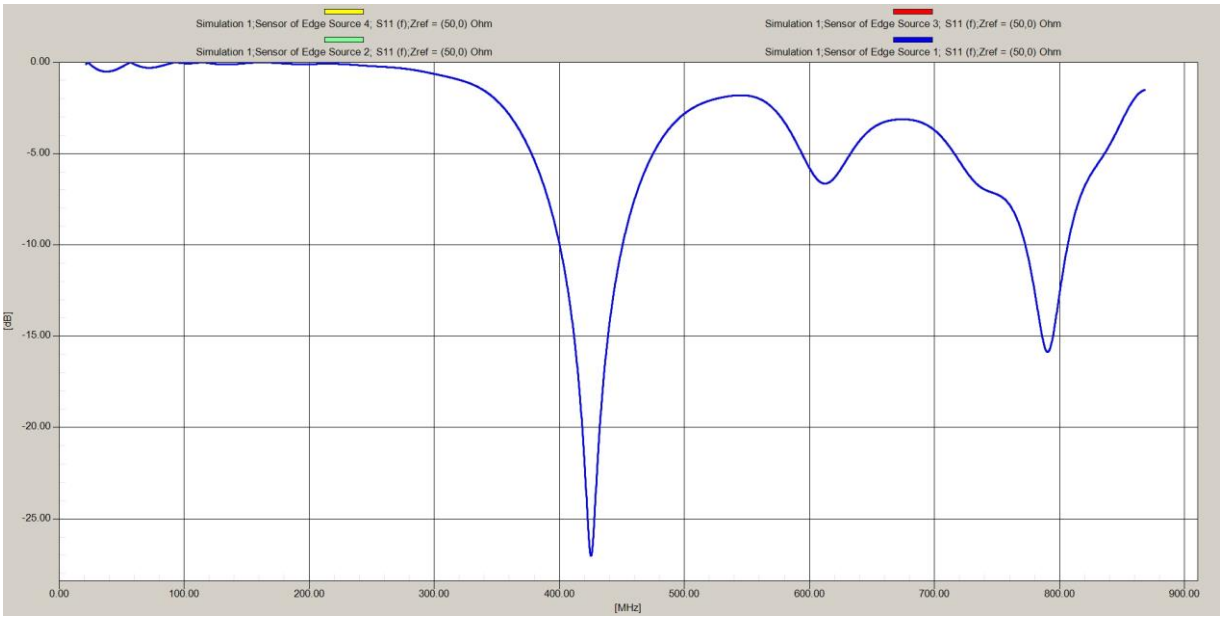

Picture 5-27 Frequency response of coefficient of reflection S_{11}, the value on desired operating frequency 434 MHz is -18,5 dB.

The minimum of S_{11} is at frequency 425,5 MHz with value -27,0 dB. On desired operating frequency 434 MHz the value achieves -18,5 dB. So impedance matching at the frequency of 434 MHz stayed the same just like in the previous case, but other waves at other frequencies are avoided more. Also distribution of the SAR stayed without significant changes.

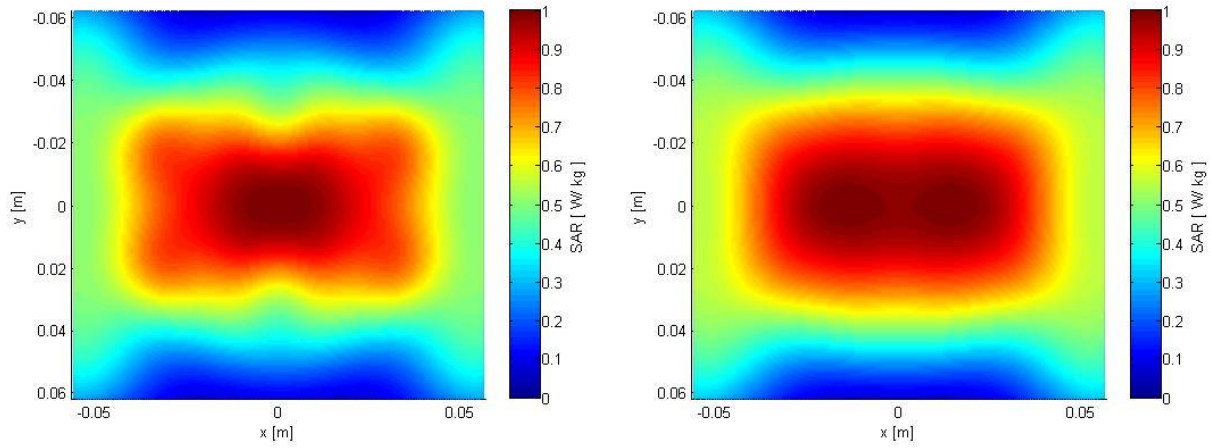

Picture 5-28 a) (left) SAR - Specific absorption rate on the surface of skin and b) (right) in the depth 1 cm under the surface of skin

We can see in the previous figures (Picture 5-25 a) and b)), that the area of radiation is homogenous in both cases as in the previous model.

In the following chart (Picture 5-29) you can see the comparison of results of coefficient of reflection S_{11} in the three previous cases. The green line represents narrowing of the gap between the slots along the axis Y about 8 mm to 9,62 mm, the blue line represents narrowing about 11 mm to 6,62 mm and the red line represents narrowing about 13 mm to 4,62 mm between the slots along axis Y.

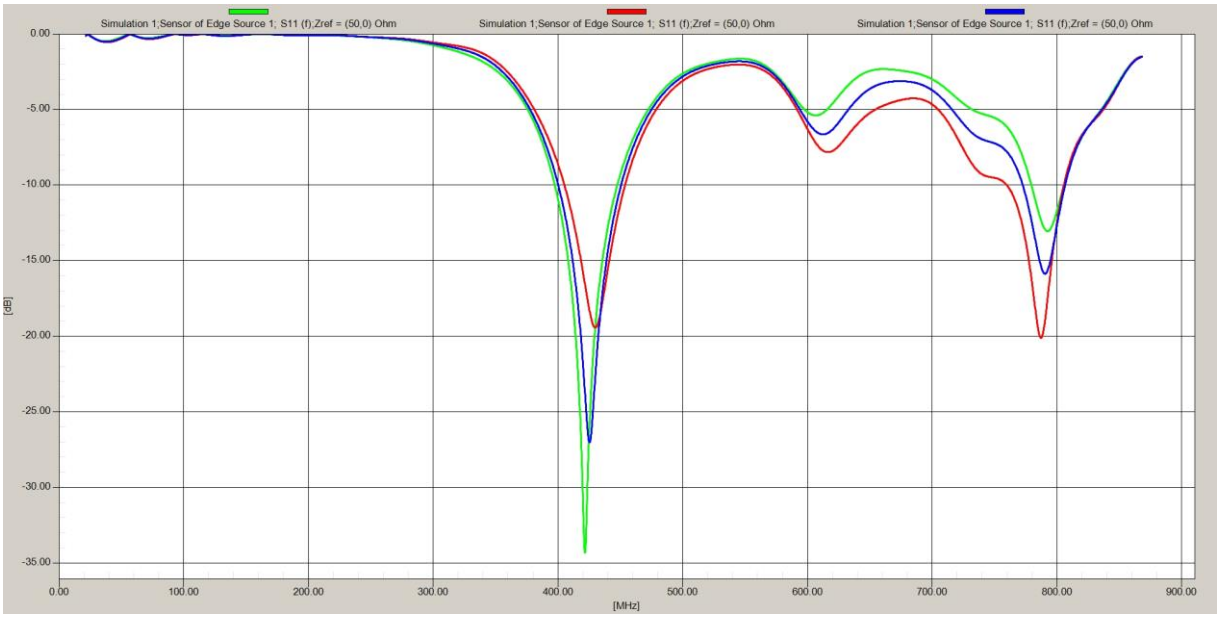

Picture 5-29 Frequency response of coefficient of reflection S_{11} – green line: gap 9,62 mm, -16,0 dB at 434 MHz; blue line: gap 6,62 mm, -18,5 dB at 434 MHz; red line: gap 4,62 mm, -18,5 dB at 434 MHz.

We can notice that the green line has the deepest peak of S_{11} but also at the lowest frequency, at the frequency 434 MHz achieves the value -16 dB, which is sufficient. The other two lines, however, achieve better value -18,5 dB and moreover, the distribution of the SAR for model represented by the green line is not completely homogenous, as shown above. On the other side, when we compare models represented by the lines blue and red, both of them achieve value of S_{11} -18,5 dB and also both of them have homogenous distribution of SAR on the surface of skin as well as 1 cm under the surface of skin. Nevertheless, here is easier to notice the above-mentioned difference between courses of the frequency responses of these lines. In regard to blue line we can say, that the attenuation close to the desired operating frequency is substantially deeper and more significant than the peak of harmonic waves. As to the red line we must conclude, that both waves achieve approximately the same value, this means that both of them are equally significant and this fact could have impact of course on the measurement and the measured data.

Based on the above mentioned analysis, I decided to use as the final model of matrix of four quadrants the model represented by the blue line with width of gap between the slots 6,62 mm. This model will be described in detail in the following section of my thesis.

5.4.1 Final matrix of four quadrants

As I wrote in previous chapters, my final model is represented by the matrix of four same quadrants. First, I optimized this quadrant separately, as it can be seen in chapter "Optimization of one quadrant of applicator in SEMCAD", and further I created matrix from this quadrant and I did a number of adjustments until I received the final model. This process of work can be seen in the previous section of this chapter.

Because the composition of the quadrants into matrix hadn't significant effect on course of S_{11}, I tried to modify the model so as to obtain a homogeneous distribution of SAR, as I described above I achieved this by using approximation of slots along one axis. Therefore, logically the final model is not regular square shape, but rectangle. All dimensions of model are listed in the following table (Table 4).

structure	dimension (mm)
the length of the central axis of the slot	115,60
width of gap	1,00
edge length, axis X	113,00
edge length, axis Y	124,00
plating thickness	0,03
thickness of substrate	1,50
radius of inner metalized circle's sector	32,13

Table 4 Dimensions of the final model.

Because the matrix is composed of four quadrants, and each of them is excited through one source, the resulting model it is excited through four sources.

The values of parameters used for the simulation of applicator and the specified in program SEMCAD are identical to the parameters used for the simulation of a single quadrant, but for the completeness, mention again in the following table (Table 5).

material	relative permittivity ε	conductivity σ (S/m)	density ρ (kg/m^3)
dielectric substrate (kuprextit)	4	-	-
biological tissue	54	0,8	1050
distilled water (bolus)	81	-	1000

Table 5 Values of parameters used for the simulation[17].

In a simulator SEMCAD I created a three-dimensional model, which you can see in the following picture (Picture 5-30) and to each structure I assigned properties and parameters mentioned in table above.

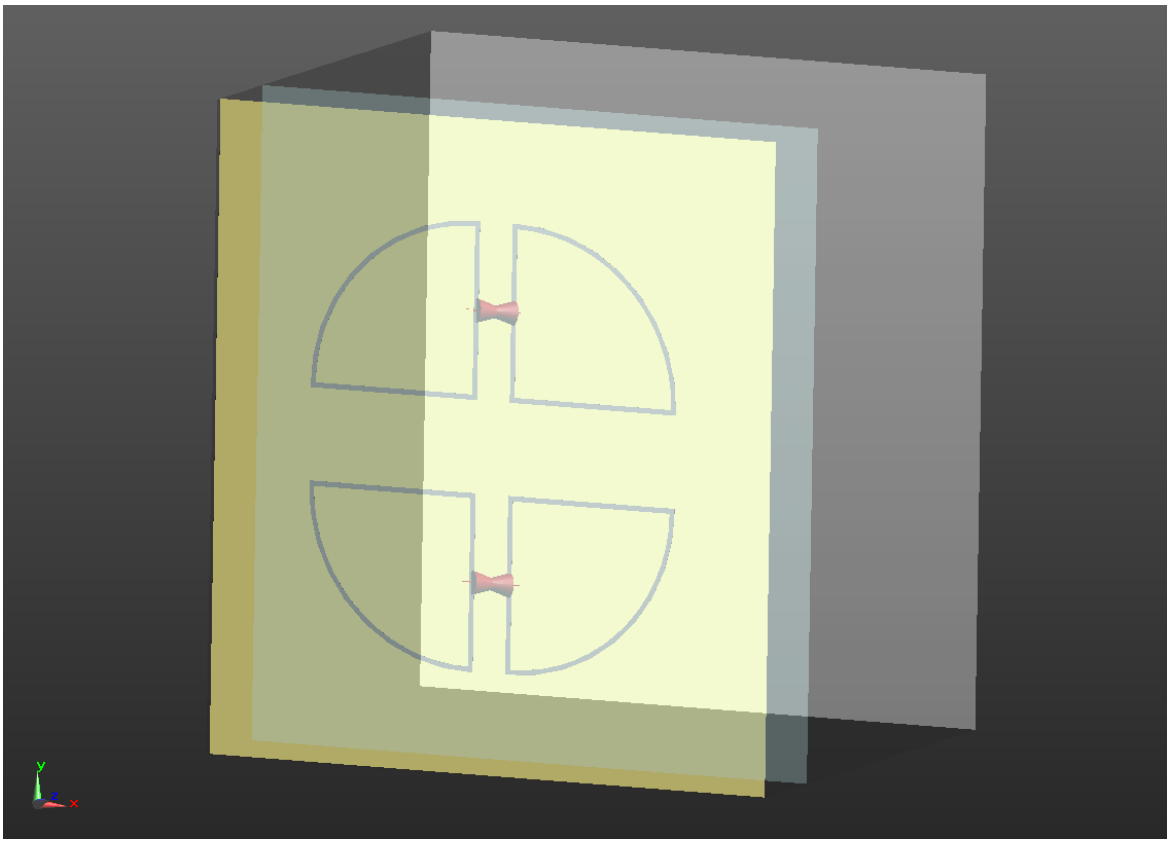

Picture 5-30 Model of matrix in an environment of simulator SEMCAD.

Following that I checked the results including duration of propagation of waves in the environment and distribution of intensity of electromagnetic field *E*. In the following picture (Picture 5-31) there is animation shot from of distribution of *E* as an example.

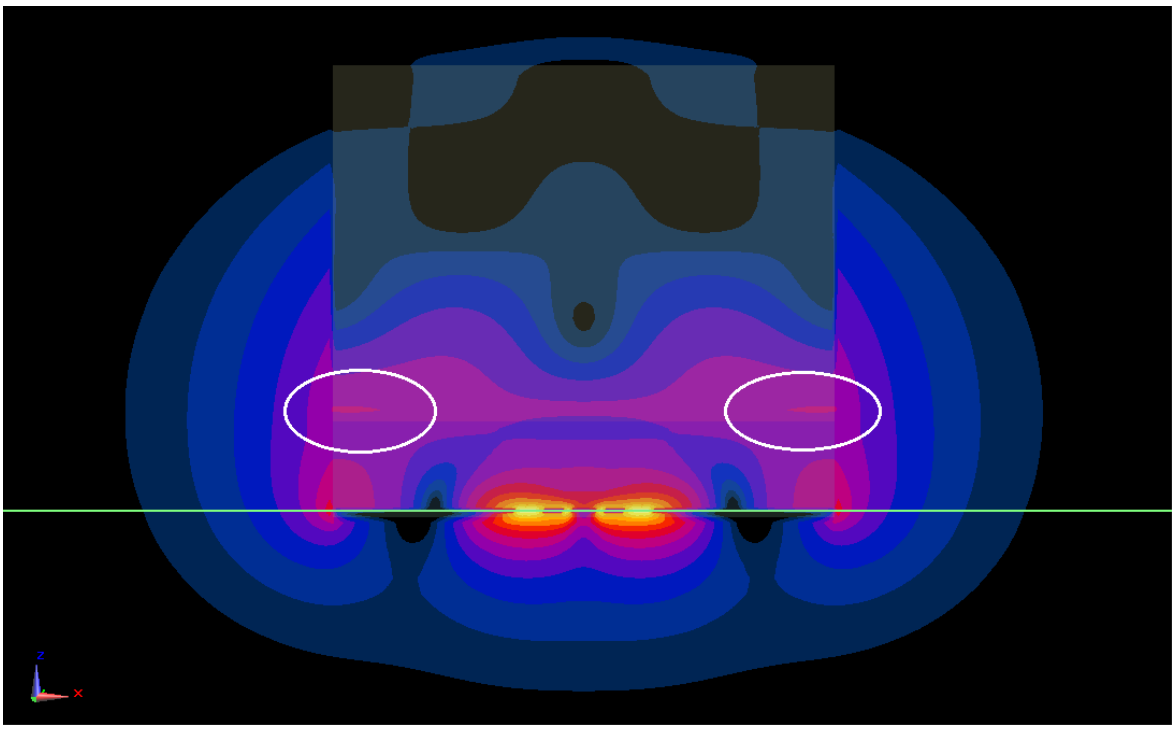

Picture 5-31 Duration of intensity of electromagnetic field *E*.

As it can be seen at the edges of agar, there is an apparent reflection of waves and a formation of standing waves. I marked these critical points by white ellipses. We could notice this phenomenon already in the picture of distribution of the SAR (Picture 5-28 a)) in last part of this chapter, but it is more evident in this particular visualization.

Formation of standing waves has significant impact on all others results. Therefore, I enlarged water bolus and agar by two centimeters on all sides, as shown in the following picture (Picture 5-32). The result of this step can be seen below in the picture of duration of intensity of electromagnetic field *E* by model with extended water bolus and agar (Picture 5-33). As we can notice, there is no reflection of waves and there are no standing waves, which could have impact on all others parameters such as coefficient of reflection S_{11}, distribution of the SAR or effective penetration depth, for clarity I marked the critical points, now without reflections, by white ellipses again.

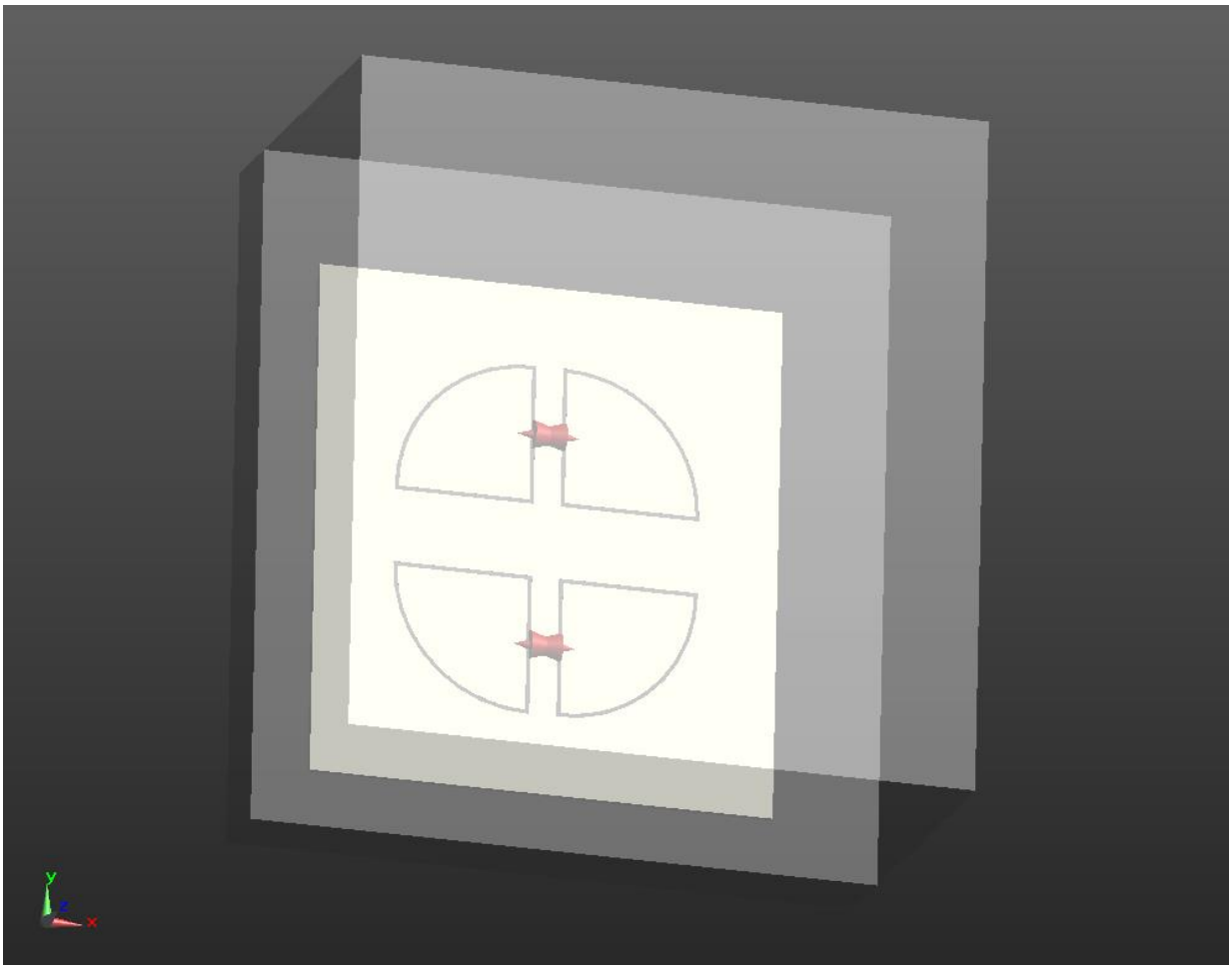

Picture 5-32 Model of matrix in an environment of simulator SEMCAD with extended water bolus and agar.

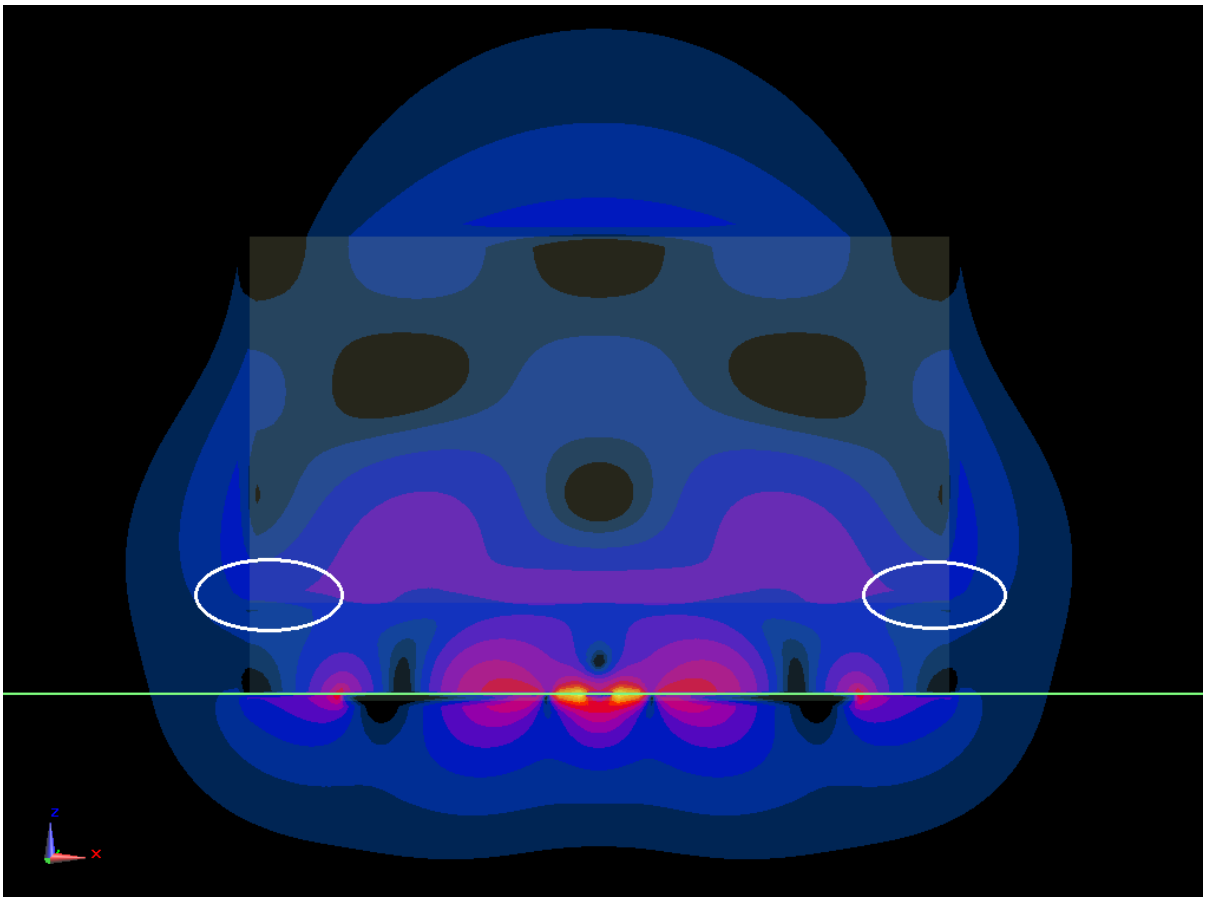

Picture 5-33 Duration of intensity of electromagnetic field *E* by model with extended water bolus and agar.

5.4.1.1 Coefficient of reflection S_{11}

In the following chart (Picture 5-34) we can see course of frequency response or coefficient of reflection S_{11} of final model. Because there is only one line, it is clear, that all sources have identical course of S_{11}. We can notice two peaks or two minimums. The deeper peak has minimum at frequency 425 MHz with value -14,2 dB and at our desired operating frequency 434 MHz achieves -12,2 dB. The harmonic wave, which we can see in the right part of the frequency spectrum close to 800 MHz, is not very significant and should not have effect on the future practically measured results.

It can be concluded that this impedance matching at operating frequency is satisfactory. Value of the ratio of standing waves achieved 1,64, thus less than 2 as it was specified in the work assignment.

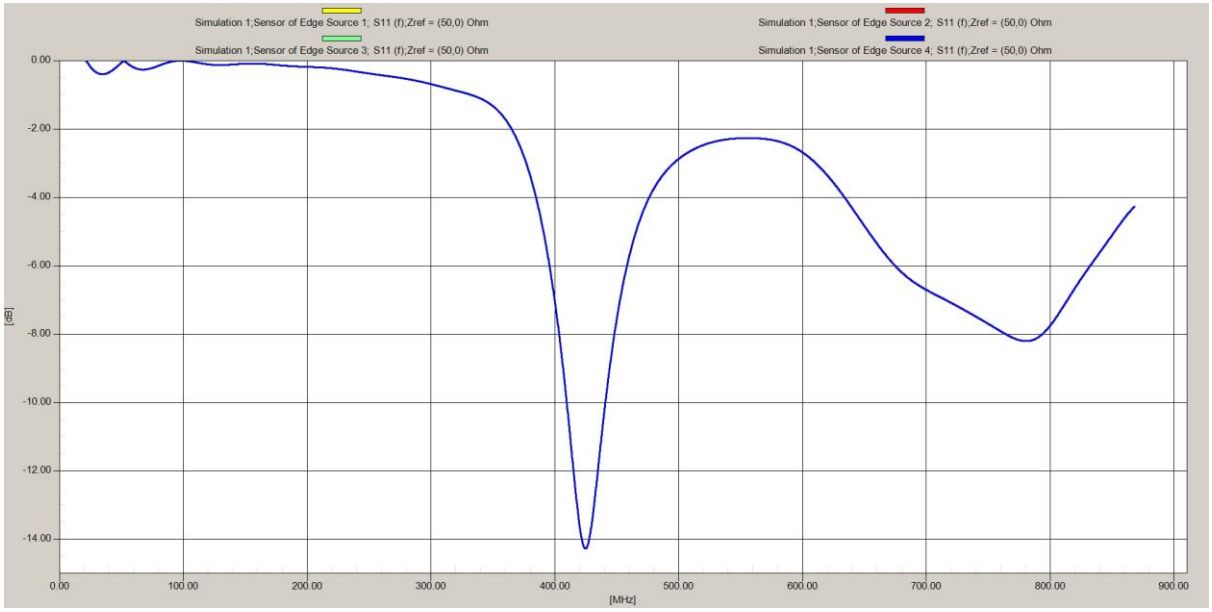

Picture 5-34 Frequency response of coefficient of reflection S_{11}, the value on desired operating frequency 434 MHz is -12,2 dB.

Also there is a difference between frequency response of S_{11} by model with smaller water bolus and agar in the chart (Picture 5-27) and this chart above (Picture 5-34) referring to the model with extended water bolus and agar. In this case, there is a decline in value of -18,5 dB to -12,2 dB.

5.4.1.2 Effective aperture – distribution of specific absorption rate – SAR

The distribution of the SAR was changed by impact of extended the water bolus and agar, as well. This result becomes by comparing the figure (Picture 5-28 a)) and the new following figure (Picture 5-35). Here, the area of penetration has the shape of number 8. It can be concluded, that is homogenous area with one focus in the middle of effective aperture, for better imaging, how is formed focus in depending on the position of the slots, I drew with black line inside shapes of slots as in the case of one quadrant.

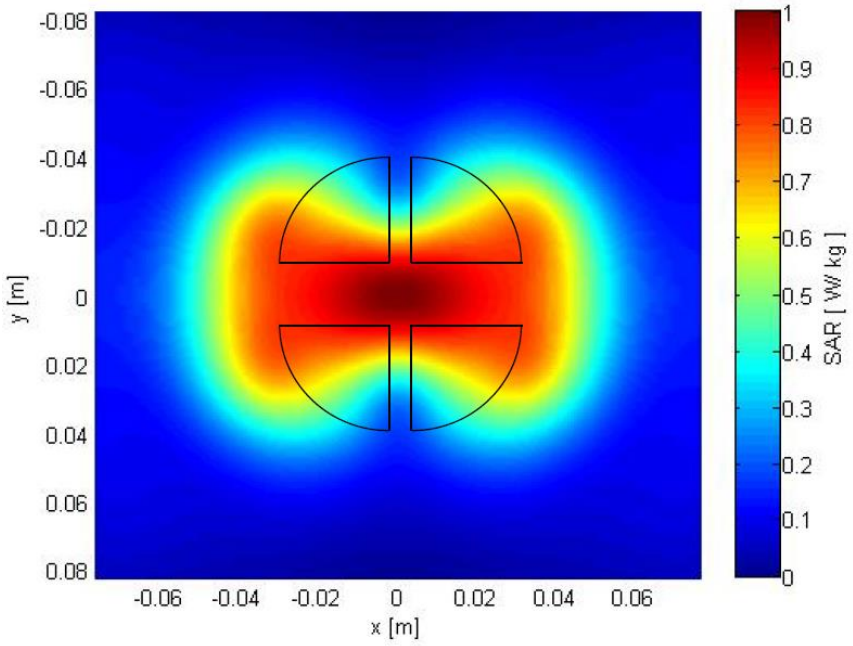

Picture 5-35 SAR - Specific absorption rate, on the surface of skin with shapes of slots.

In the figure of distribution of the SAR in the maximum (Picture 5-36), focus has shape of number 8 as well but has two focuses. Still, we can say, that this distribution in the maximum SAR is homogenous.

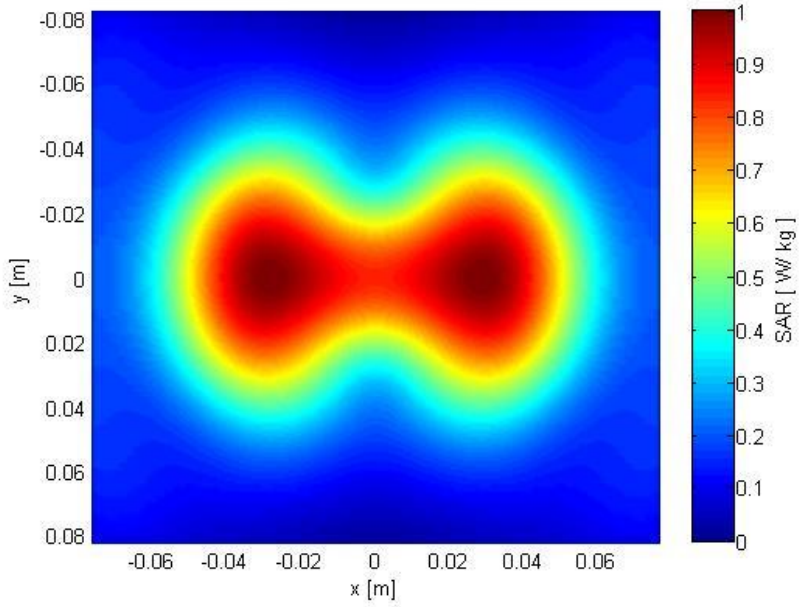

Picture 5-36 SAR - Specific absorption rate, 1 cm under the surface of skin

5.4.1.3 Effective penetration depth

In the views of effective penetration depth (Picture 5-37) and (Picture 5-38) was reflected the oval shape of distribution of SAR with two focuses in bigger depth of penetration. In case of axis Y we can see penetration almost along all length of applicator, in the other case we can see increase the absorbed power into depth only in the middle of structure.

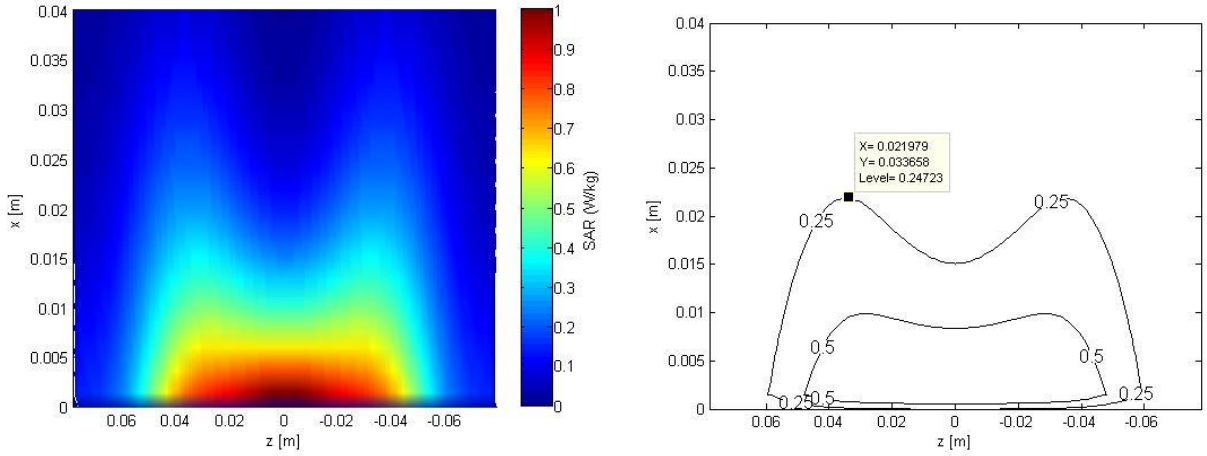

Picture 5-37 Effective penetration depth of final matrix – axis Y a) slice in axis Y, b) contours of 50 % and 25 % of value of SAR.

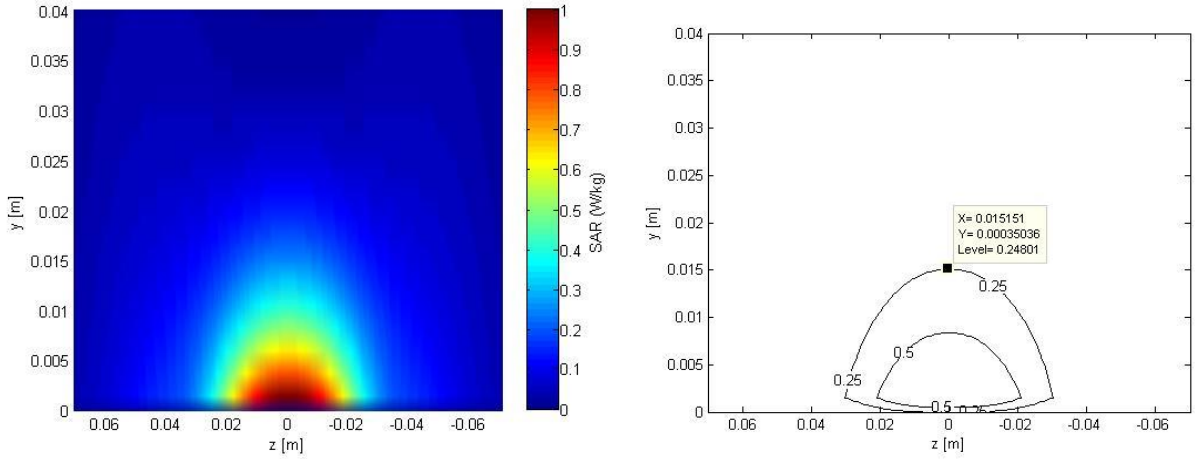

Picture 5-38 Effective penetration depth – axis X slice in axis Y, b) contours of 50 % and 25 % of value of SAR

In first cases the value of effective penetration depth achieves about 2,1 cm, in second case seems this value achieves about 1,5 cm, as can be seen in the pictures (Picture 5-37 b)) and (Picture 5-38 b)).

In the next picture (Picture 5-39) of this model we can see distribution of the SAR in effective penetration depth, thus in depth which corresponds with decline in value by 50 % from value in depth 1 cm under the surface of skin, it is the same views as in case of one quadrant, value of effective penetration depth in this case 2,1 cm. At this depth are evident two focuses.

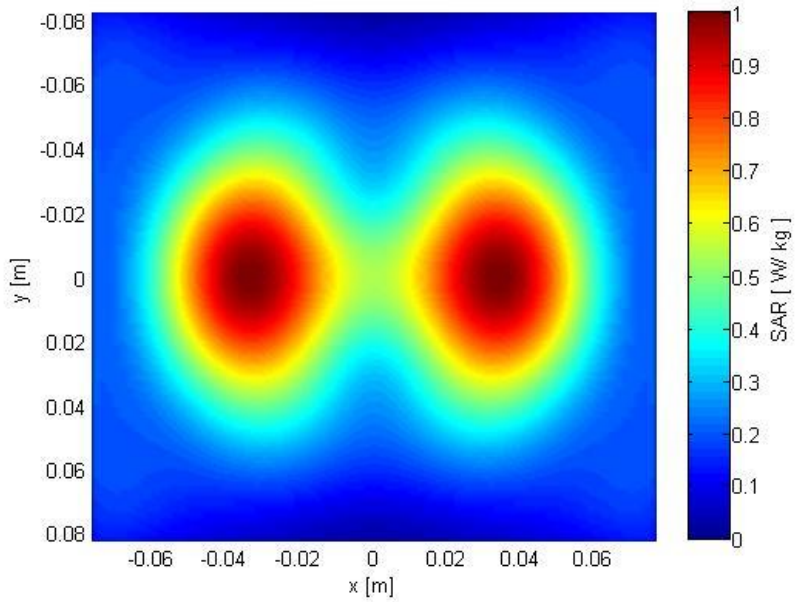

Picture 5-39 SAR - Specific absorption rate, 2,1 cm under the surface of skin in effective penetration depth with shapes of slots.

5.4.1.4 Comparison of matrix with one quadrant

As the last comparison in this work, I would like to compare at least some of the previously monitored parameters between one quadrant and the resulting matrix of quadrants.

In the following chart (Picture 5-40) there are two courses of frequency responses or coefficients of reflection S_{11}. The red line represents courses of S_{11} of quadrant and the other blue line represents courses of S_{11} of matrix of quadrants. We can also notice that in case of matrix the minimum of S_{11} at frequency 434 MHz achieves lower value (-12,2 dB) than by one quadrant (-18,5 dB), as well at higher frequencies the course of the S_{11} by one quadrant looks better, the harmonic wave has pronounced minimum, but at higher frequency. Nevertheless we can say that results of practical measurement will not be affected by interference.

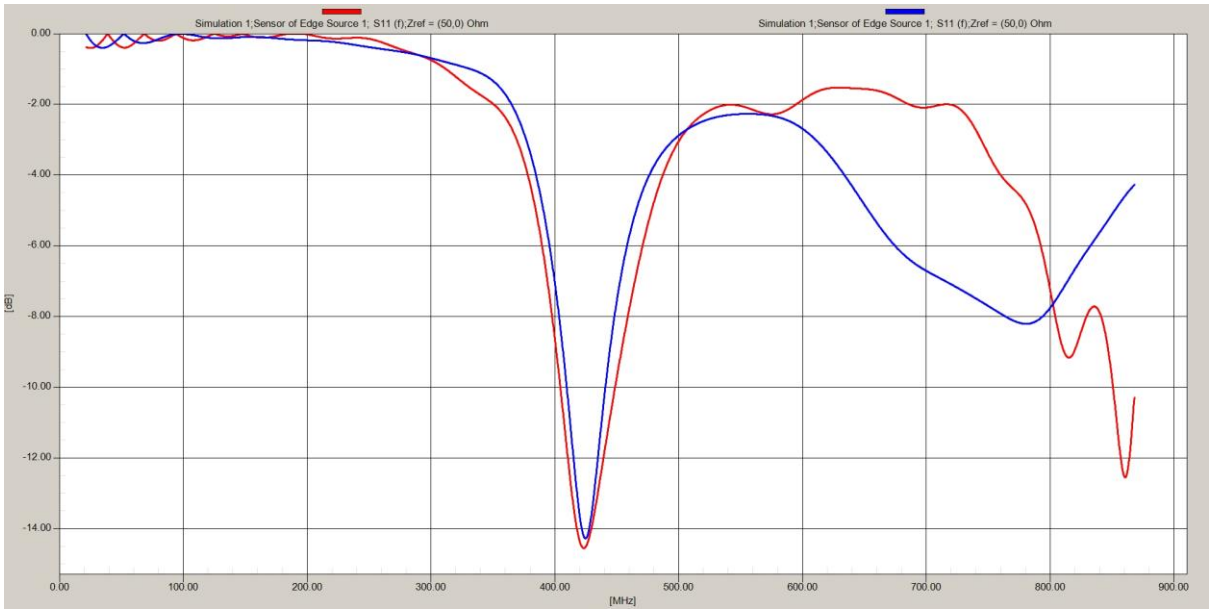

Picture 5-40 Frequency responses of coefficients of reflection S_{11} – red line: one quadrant -18,5 dB at 434 MHz; blue line: matrix of quadrants -12,2 dB at 434 MHz.

The effective penetration depth is approximately similar, to the analysis I performed with results of contours from MATLAB in the following pictures (Picture 5-41 a) and b)) and (Picture 5-42 a) and b)).

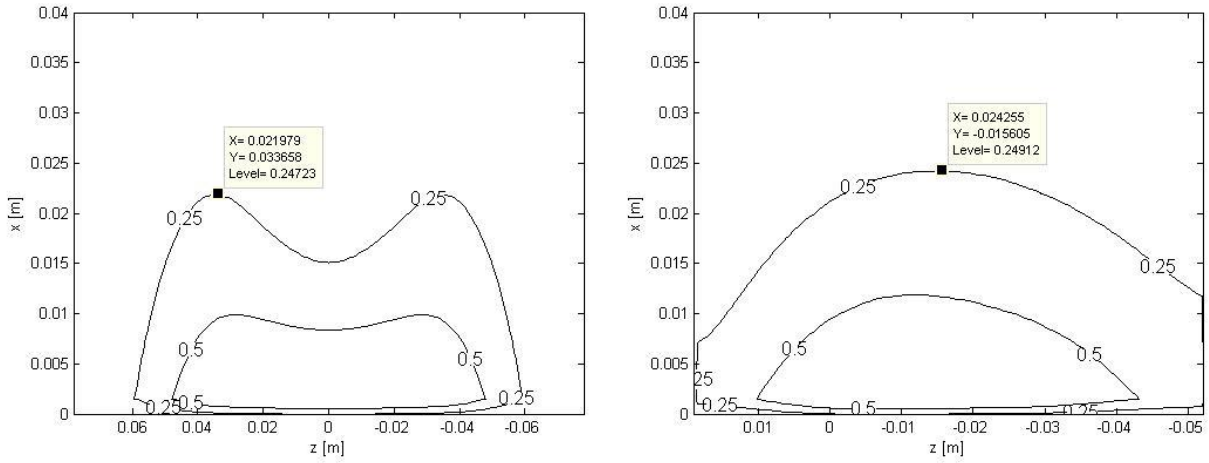

Picture 5-41 Comparison of the effective penetration depth – axis Y a) (left) final matrix, b) (right) one quadrant.

In the charts contours of the effective penetration depth of axis Y above can be seen, that in both cases the effective penetration depth, the curve of 25 % of value, achieves higher value than 2 cm. In the case of matrix the value achieves almost 22 mm, exactly 21,97 mm, in the case of one quadrant the value achieves more than 24 mm, exactly 24,25 mm.

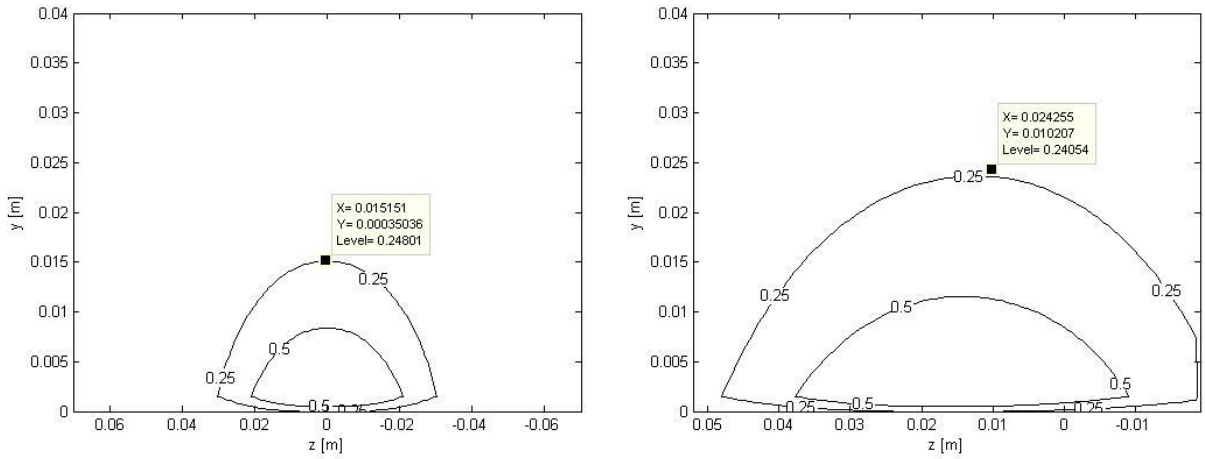

Picture 5-42 Comparison of the effective penetration depth – axis X a) (left) final matrix, b) (right) one quadrant.

Also in the charts (Picture 5-42 a) and b)) can be seen values of effective penetration depth. We can see that in the case of matrix the maximum of 25% curve achieves value only about 15 mm. It corresponds to chart of effective penetration depth of matrix of axis Y above, we can notice that in the middle of radiation of matrix the shape of radiation is narrower and lower. In the case of one quadrant the charts of both axes seem similar, the radiation has shape of hill, which is symmetric in both axes.

5.5 Implementation of a planar applicator

Implementation of applicator was carried out in premises of Faculty of Electrical Engineering CTU in Prague. I manufactured the applicator separately under professional supervision and assistance.

The applicator consists of dielectric substrate Cuprextit which value of permittivity ranges from 4 to 5,5. It is used in electrical engineering as insulating material or as a substrate for prediction of the printed circuit board PCB for the attachment of electrical components. It is phenyl- formaldehyde resin, hardened paper or glass fabric (similar laminate) [13]. It has a low thermal expansion coefficient, has excellent dimensional stability and therefore is reliable even under severe temperature conditions. The board is 1,5 mm thick, plated on one side and the plating thickness is about 30 to 35 microns [13].

I used the AutoCAD program to create the technical drawing of applicator, which I used as a template for the manufacturing of the board by company PragoBoard s. r. o.

Such a board required four connectors according to the design in the simulator SEMCAD. I made holes with drill at specific points having a radius of 1,3 mm for central conductors of connectors SMA, which I subsequently soldered to the internal structures of the applicator. For right function of applicator it was necessary to electrically connect the grounding plating (outer square) with the outer conductor of connectors. I achieved this by soldering the copper wire on the ground side of the structure and on the other side with the outer conductor of the connector.

The final form of the applicator can be seen in the picture (Picture 5-43) below.

Picture 5-43 Final applicator, left - front side, right - back side.

Technical drawing of produced applicator is attached as an annex at the end of the thesis.

6 Practical measurements with applicator

The applicator was designed and adapted in ideal and precisely defined conditions, with ideal characteristics and precision in an environment of simulator SEMCAD. The production itself, however, could cause inaccuracies. Real applicator did not have to work as said the program before. It was one of numerous reasons, why it was necessary the properties of applicator empirically verified by measurement. Of course, I intended to get proper data for processing, analyzing and concluding my work. Measurement was performed at the Faculty of Electrical Engineering Czech Technical University in Prague under the expert supervision of thesis's supervisor.

The most important parameters which I wanted to check were the reflection of coefficient S_{11} and the SAR distribution in the agar. For the first measurement I used the microwave analyzer Agilent of type E5062A, measuring in the range of 0,3 - 3 GHz. To verify the temperature distribution in the agar after exposure by the applicator I used UHF-power-generator PG 70.150.2, both devices you can see in the picture (Picture 6-1 a) and b)) below.

Picture 6-1 a) (left) UHF-power-generator PG 70.150.2, b) (right) microwave analyzer Agilent.

6.1 Preparation of agar phantom

Agar phantom is a model of biological tissue which has the same dielectric and thermal parameters as human tissue (human muscle) [17]. The parameter conductivity is very dependent on salt concentration which we use during cooking. We can prepare agar from seaweed powder, usually we use 40 g of agar powder on 1l of water and we add 3g of salt [15]. This mixture is then cooked for 15 minutes, as you can see in the picture (Picture 6-2), and then let it go. While transferring material into the container we must avoid bubbles. They can cause inhomogeneous parts inside of agar.

Picture 6-2 Cooking process of agar

6.2 Measurement of reflection coefficient S_{11}

This coefficient tells us, how good impedance matching this resonant circuit has. In the SEMCAD program I achieved value S_{11} -12,2 dB at 434 MHz, considering the required minimum value -10 dB. The problem of planar applicators is the fact that after manufacturing of the applicator is not possible to modify the impedance matching more in contrast to waveguides, where we can modify it for example by changing the position of the source probe or by using a transformer. In case of planar applicator we have only one possibility, we can manufacture the product again.

In the following pictures (Picture 6-3 a) and b)) there is the entire involvement of applicator with a simple power divider, also used cables had important impact of results. Therefore, it was necessary to use a minimum amount of transitions and cables.

The process and course of the measurement can be found in the picture below (Picture 6-3 c)). We can say that the measurement was successful, because the reflection coefficient S_{11} surpassed value -11 dB.

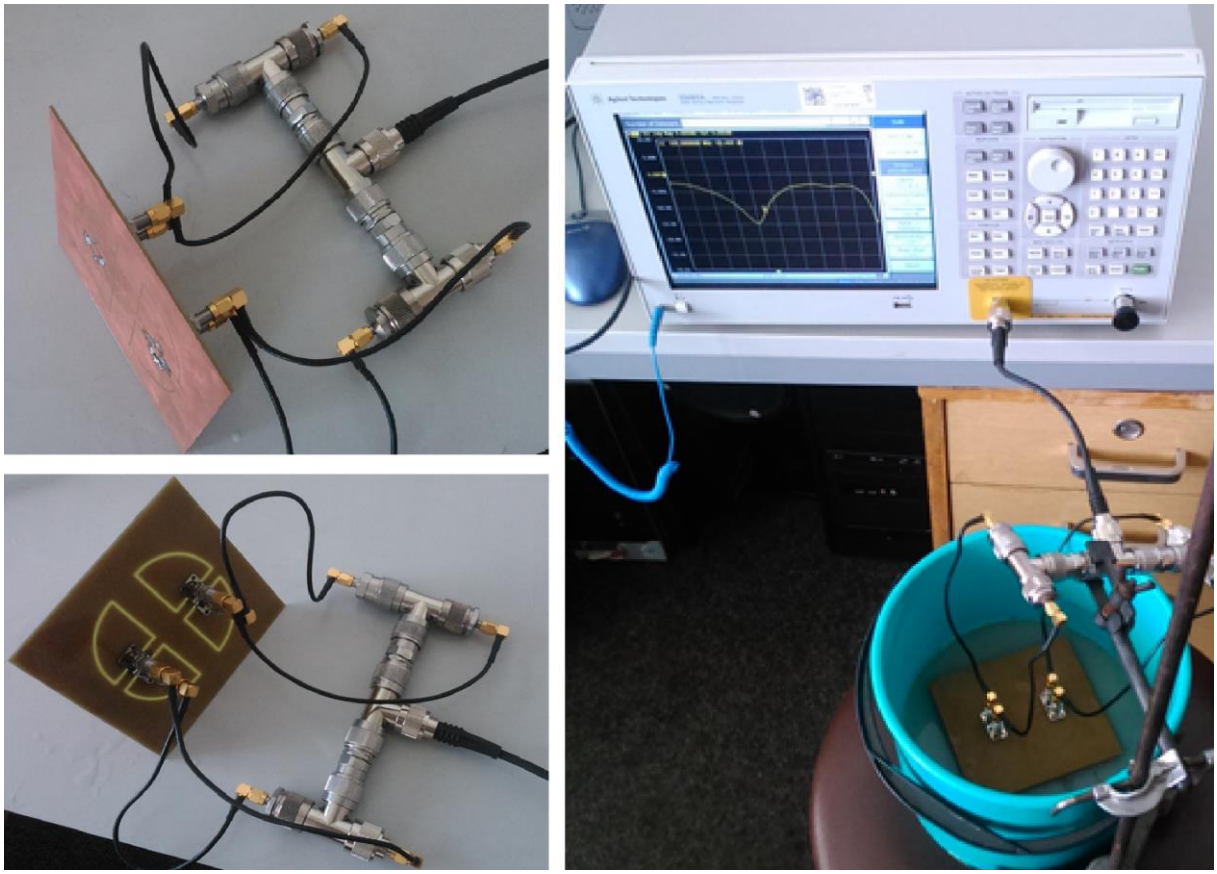

Picture 6-3 a) (left up) involvement of applicator, b) (left down) involvement of applicator, back side, c) (right) course of the measurement

In the following charts (Picture 6-4) and (Picture 6-5) there are two curves of frequency response of coefficient of reflection S_{11}. In the first chart is curve of coefficient of S_{11} was calculated by SEMCAD simulator, in the second chart is curve of coefficient of S_{11} was measured by the analyzer Agilent during the measurement with my own applicator. I created the graph from the measured values using the MATLAB.

As we can see that both curves have very similar shape. In the first case of curve calculated by SEMCAD there is a deeper peak with minimum at frequency 425 MHz with value -14,2 dB and at our desired operating frequency 434 MHz achieves -12,2 dB. In the other chart there is a minimum of the S_{11} -14,8 dB at 420 MHz and at our desired operating frequency 434 MHz achieves -11,1 dB. However, we achieved a value that exceeded -12.5 dB during the measurement.

It can be concluded that this impedance matching of manufactured applicator at operating frequency is satisfactory. Considering the very similar results of calculation of the SEMCAD simulator and measurement using analyzer Agilent also we can say that the measurement was successful and we demonstrated the proper functioning of the applicator.

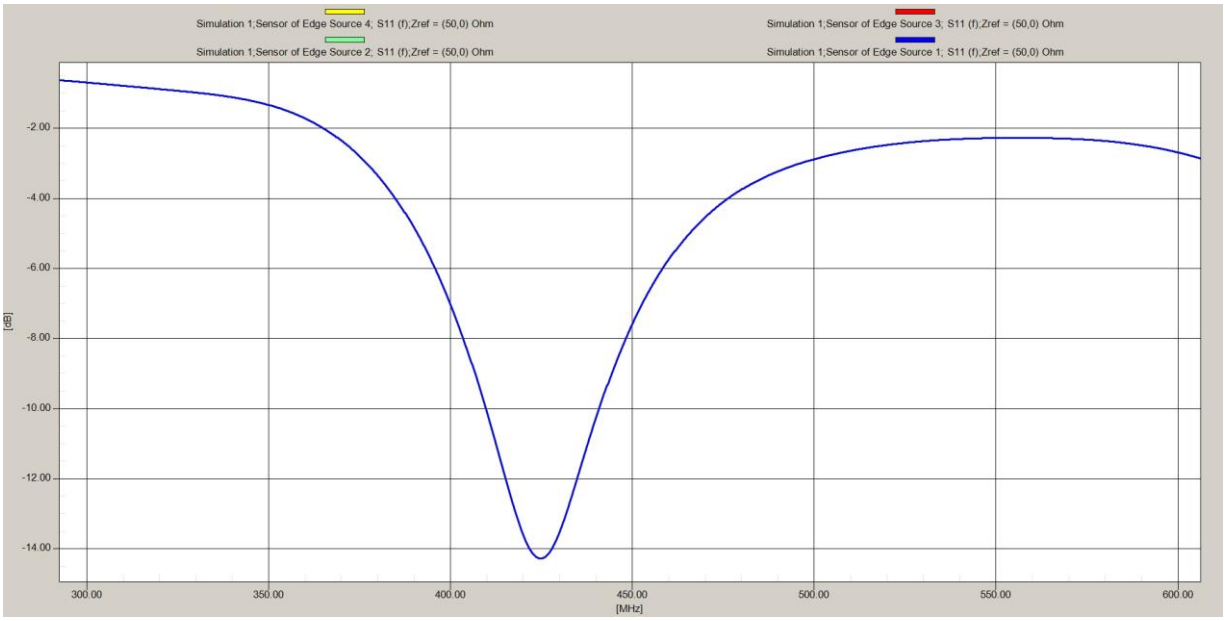

Picture 6-4 Course of coefficient of reflection S_{11} calculated by the SEMCAD simulator (on axis X – frequency, on axis Y – dB).

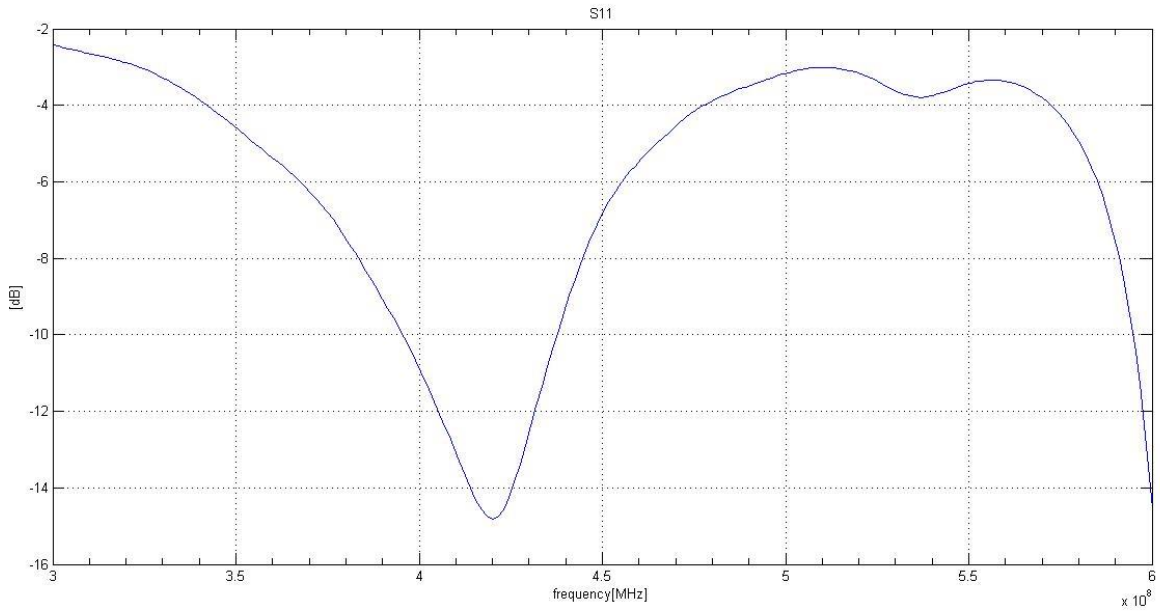

Picture 6-5 Course of coefficient of reflection S_{11}, which was measured (on axis X – frequency, on axis Y – dB).

6.3 Numerical and empirical verification of the SAR distribution into the agar phantom

Considering the good results of previous measurements, where we verify the correct impedance matching, it is possible to continue with measuring of the distribution of the SAR into agar. For that I needed above all mentioned power generator and a thermal imager FLIR P25 (possible measured temperature range is -40 °C - 120 °C). Agar phantom had to have temperature of the ambient air for the correct and undistorted capture of temperature increased by thermal imager. The process of measurement of distribution of the SAR is shown below (Picture 6-6). Applicator was connected with water layer, water bolus, and the microwaves were routed through the water into the agar. The control panel power generator was set to the power of 100 W and we started heating for about 7 minutes.

Picture 6-6 Measuring of the distribution of SAR into agar, (left) power generator with applicator, (right) thermal imager FLIR P25

After completion of the heating, we removed the applicator from agar phantom and we focused the thermal imager on irradiated area. In the following pictures (Picture 6-7), (Picture 6-8) and (Picture 6-9) are photos taken during and at the end of irradiation.

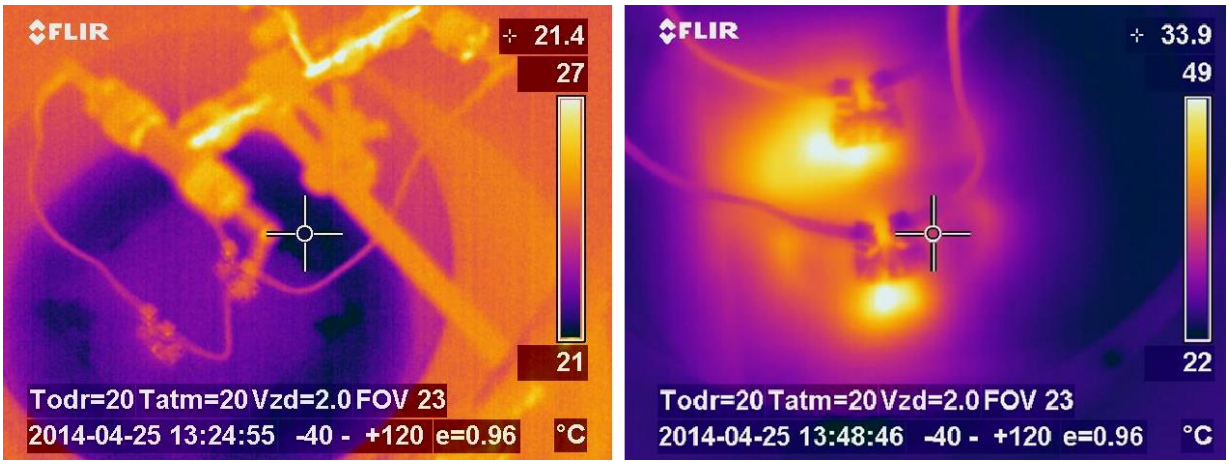

Picture 6-7 View of the applicator during the heating.

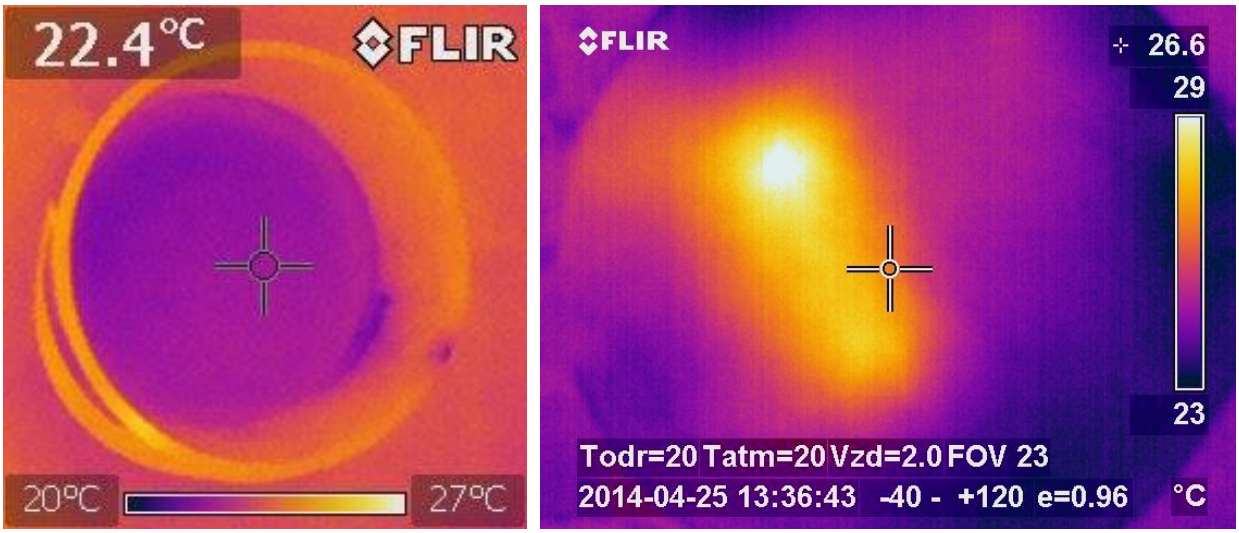

Picture 6-8 View the agar surface a) (left) before the heating and b) (right) after the heating.

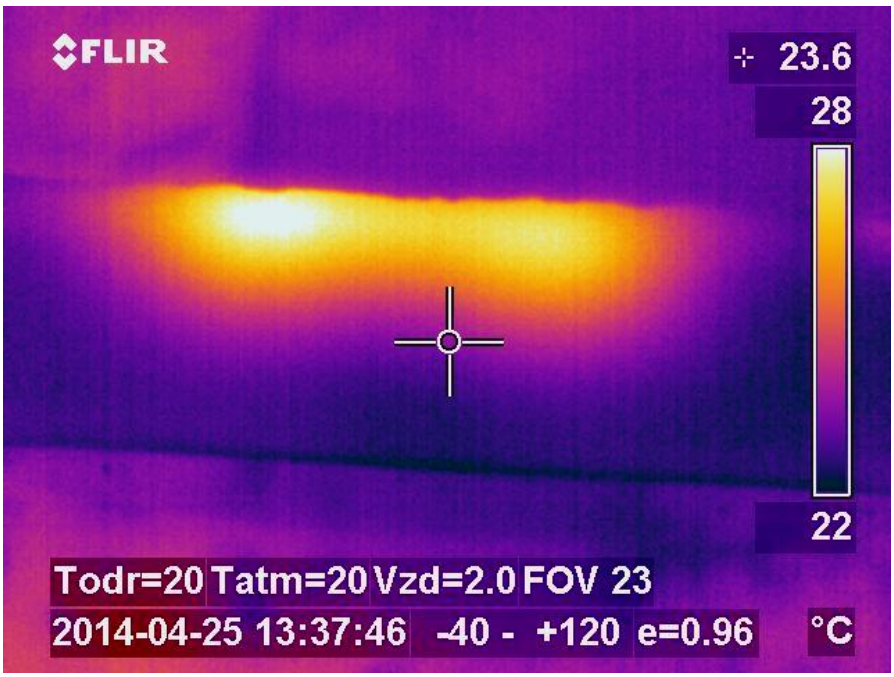

Picture 6-9 Cross-sectional view of agar heated by planar applicator after about 7 minutes of heating.

6.4 Calculation of the SAR distribution from the measured thermograms

For mathematical verification and calculation of the SAR distribution in the agar I used thermal images obtained with a thermal imager. For calculation we used equation (4th 19), heat conduction in the body are neglected:

$$SAR = c \cdot \frac{\Delta T}{\Delta t} \qquad (6.\ 1)$$

Where c is the capacity of human tissues (c = 3100 J kg^{-1} K^{-1}), ΔT is the temperature change, which I deducted from the thermogram Picture 6-7 (ΔT = 6) and Δt indicates the period during which ran heating (t = 7 min = 420 s).

Upon substituting the above values into the equation (6. 1) we obtain the final value of the SAR distribution in the agar at the point of greatest intensity:

$$SAR = 3\ 100 \cdot \frac{6}{420} = 44{,}28\ \text{W/kg}$$

7 Conclusion

The task of my thesis was to get acquainted with the topic of medical oncology method "hyperthermia". Briefly discuss the impacts of electromagnetic field on biological tissue, the types of planar applicators for superficial treatment and the types of waves which can be propagated in the applicator. Further the parameters which can be used for description of conduction, as well. Than in the SEMCAD simulator design and optimize planar applicator at the operating frequency of 434 MHz. Finally, as a last step, manufacture and measure properties and features of this applicator.

I obtained enough information about hyperthermia from references, which are mentioned at the end of this work but the most knowledge I obtained during creating my bachelor thesis. Therefore, I could briefly but clearly and concisely summarize the current knowledge about the effects of electromagnetic fields on biological tissue and the principle of treatment using hyperthermia. I described planar applicators and I analyzed the various lines, which are among the planar structure. I mentioned waves, which are propagated in these structures and I described parameters, which can be used for description of conduction.

In the beginning of the practical part of my work I tried to demonstrate, how much important is number of voxels, which we use for simulation in the SEMCAD simulator. The result can be found in the subchapter "5.2.1. Influence of number of voxels" and it can be concluded that impact of number of voxels on course of the coefficient S_{11} and the SAR is very significant. In the following subchapter "5.2.2. Influence of shape of slot on the results" I compared two models, which have only one difference, the shape of the slot. Also in this case we can notice difference between courses of the S_{11}, distribution of the SAR and also between effective penetration depths, where is the most evident difference. In the case of the square shape was the value of effective penetration depth about 7 mm higher than in the case of the circular sector slot.

As next step I optimized one quadrant of final applicator. The results and workflow can be found in the subchapter “5.3 Optimization of one quadrant of applicator in SEMCAD”. Concerning the value of coefficient of reflection S_{11} on frequency 434 MHz it reaches a value of attenuation -13,15 dB and value of the effective penetration depth achieves more than 24 mm.

The process of work of creating of final model, which I received after a number of adjustments, can be found in the subchapter “5.4 Design and simulation of the complete model of matrix of four quadrants in the SEMCAD”. The dimensions of applicator can be seen in the table (Table 4). The value of the coefficient of reflection S_{11} at desired operating frequency 434 MHz achieves -12,2 dB and value of effective penetration depth achieves 21,97 mm. I also compared matrix and one quadrant at the end of this part of work. It can be concluded that in both cases the impedance matching is satisfactory and values of effective penetration depth achieve more than 21 mm, it can be considered as successful.

In the last chapter “6 Practical measurements with applicator” it can be found the workflow of practical measurement and also results, which were measured by using my one applicator manufactured on the Faculty of Electrical Engineering. At desired operating frequency 434 MHz the value of the S_{11} achieves -11,1 dB. The effective penetration depth of final model can be seen in the pictures of thermographs. Thickness of the irradiated phantom was more than 5 cm, therefore I estimate from thermographs that the effective penetration depth was about 25 mm. The temperature increased about 6 degrees after 7 minutes of heating from 22 °C to 28 °C. The value of distribution of the SAR in the place of the highest intensity, which I calculated, is 44,28 W/kg.

References

[1] Kejzlarová, N.: *Planární aplikátory pro podpovrchovou léčbu*. (Planar applicator for subsurface treatment) Bacherol thesis., Prague, 2011

[2] Vrba, J.: *Lékařské aplikace mikrovlnné techniky*. (Medical applications of microwaves) Textbook CTU in Prague, Prague, 2007

[3] Int. Journal of Hyperthermia, ESHO 1992 – 2008.

[4] Novotný, K., Škvor, Z., Mazánek, M., Pechač, P.: *Vlny a vedení.* (Waves and Lines) Textbook CTU in Prague, Prague, 2005

[5] Prokop, J., Vokurka, J.: *Šíření elektromagnetických vln a antény.* (Propagation of electromagnetic waves and antennas) SNTL – Publishers of technical literature, Bratislava, 1982

[6] Procházka, M.: *Antény – encyklopedická příručka.* (Antennas - Encyclopedic Guide) BEN – technical literature, Prague, 2000

[7] Kejzlarová. N., Fišer, O.: *Aplikátory pro lokální mikrovlnnou termoterapii.* (Applicators for local microwave thermotherapy) Team project, Prague, 2011

[8] Němec, L.: *Aplikátor pro termoterapii na bázi planárního rezonátoru.* (Applicator for thermotherapy based on planar resonator) Diploma thesis., Praque., 2008

[9] Vrba, J., Lapeš, M.: *Mikrovlnné aplikátory pro lékařské účely*. (Microwave applicators for medical purposes) Textbook CTU in Prague, Prague, 1995

[10] Hoffmann, K.: *Planární mikrovlnné obvody*. (Planar microwave circuits) Textbook CTU in Prague, Prague, 2000

[11] Vrba, J.: *Úvod do mikrovlnné techniky.* (Introduction to microwave technology) Textbook CTU in Prague, Prague, 2007

[12] Vysokofekvenční elektrotechnika [online]. c2011, [cit. 2011 – 5 – 20], URL: http://physics.mff.cuni.cz/kfpp/skripta/vf-elektronika/07_1.html, *Magnetrony*.

[13] Speaker shop [online]. c2011, [cit. 2011 – 5 – 20], URL: http://speakershop.cz/31-kuprextit-cuprextit, *Kuprextit.*

[14] Rozman, J. and coll.: *Elektronické přístroje v lékařství*. (Electronic devices in medicine) Academia, Prague, 2006

[15] personal consultation with Ing. Ondřej Fišer

[16] Tysl, V.: *Obvody velmi vysokých kmitočtů*. (Very high frequency circuits) Textbook CTU in Prague, Prague, 1975

[17] Fišer, O., Vrba, J.: *Orignted array of Waveguide applictors for local thermotherapy*. In 8th European konference on antennas and propagation, 2014. EuCAP 2014, pp. 2169-2172.

[18] Fišer, O., Merunka, I., Vojecková, L., Vrba, J.: *Utilization of waveguide applictors combintion for electromagnetic field focusing. Radiotechnica* 2014, 2014. RE 2014.

[19] Vrba, J., Lapeš, M., Oppl, L.: Technical aspects of microwave thermtherapy. Bioelectrochmistry and ioenergetics 48, 1999, 305-309.

[20] Fišer, O.: *Orientované pole aplikátorů pro lokální termoterapii*. (Oriented field of applicators for local thermotherapy). Diploma thesis., Prague, 2013

Attachment

The technical drawing of the applicator

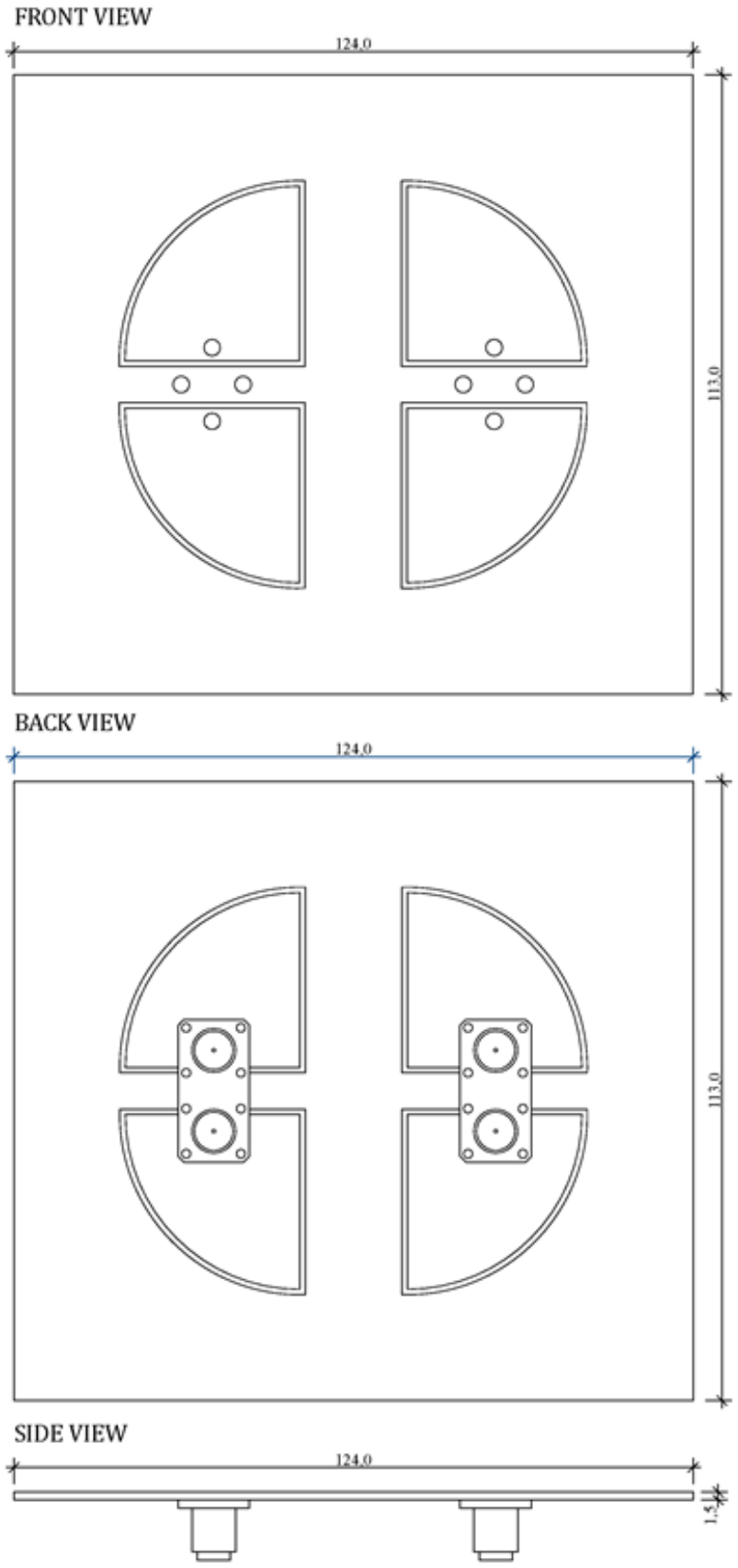

THE TECHNICAL DRAWING OF APPLICATOR 1:1